TAMPEREEN TEKNILLINEN YLIOPISTO
TAMPERE UNIVERSITY OF TECHNOLOGY

CHAUDHARY JAY KANT

EFFECTS OF USER LOCATION ON SIGNAL RECEPTION IN INDOOR LTE NETWORK

Master of Science Thesis

Examiner: Professor Jukka Lempiäinen
Supervisor: M.Sc. Joonas Säe

Examiner and topic approved by the Council of the Faculty of Computing and Electrical Engineering on 13th August 2014

ABSTRACT

TAMPERE UNIVERSITY OF TECHNOLOGY
Master's Degree Programme in Electrical Engineering
CHAUDHARY, JAY KANT: Effects of User Location on Signal Reception in Indoor LTE Network
Master of Science Thesis, 56 pages, 9 Appendix pages
November 2014
Major: Radio Frequency Electronics
Examiner: Professor Jukka Lempiäinen
Supervisor: M.Sc. Joonas Säe
Keywords: LTE, user location, indoor measurement, signal reception, received signal strength, RSRP, SNR

People spend approximately 90% of their time indoors and they expect very high quality services in every possible location. However, end users are generally not aware of the effects of their positions in the received signal levels and the performance of the system.

The aim of this research is to study the effects of user locations on received signal levels in Long Term Evolution (LTE) indoor network. With the development of some applications, users could be guided to self-optimize their User Equipment (UE) terminal to a particular position such that they will receive better connection quality. This will benefit subscribers due to the reduction in unwanted radiation and increase in battery lives. On the other hand, due to the reduction in the radio energy consumption at the Base Stations (BSs) and Mobile Stations (MSs), operators would benefit from the reduced cost and increased capacity.

In order to perform this research, the measurements were carried in the second, third and fourth floor in the Tietotalo building of Tampere University of Technology (TUT) using Nokia's LTE test network. The measurements were taken at several locations in different corridors and inside different rooms in each floor, and the measurement data were collected and analyzed using Anite's measurement software – Nemo Outdoor and Nemo Analyzer. The results are presented in terms of Cumulative Distribution Function (CDF) plots and statistical values of Reference Signal Received Power (RSRP) and Signal-to-Noise Ratio (SNR) and conclusions are derived from them.

This thesis proceeds from theoretical backgrounds on wireless communication channels to a brief introduction of LTE. This is later followed by the measurements, results and analysis, and conclusions at the end.

It was found that a slight change in the user location had a noticeable impact in the received power levels. From the experiments, it is advisable that users should position themselves in open and wider spaces and reasonably to locations where no people is moving around.

PREFACE

This Master of Science thesis has been written for the completion of M.Sc. degree in Electrical Engineering from Tampere University of Technology (TUT), Finland. The thesis works, measurements and writing process have been conducted in the Department of Electronics and Communications Engineering under the Radio Network Group.

I would like to express my genuine appreciation and deepest gratitude to my examiner Professor Jukka Lempiäinen for recommending this topic and for all his valuable advice and guidance. Sincere thanks go to my supervisor M.Sc. Joonas Säe for his constant and immense support, and constructive feedback during the whole duration of the thesis. Working under his supervision was pleasurable and motivational. Their advice helped not only completing the thesis successfully but also gave me valuable experiences and knowledge that surely prove to be an important milestone in the future as a professional wireless communication engineer. Their generous treatment and kind patience turned this thesis from a heavy burden to an exciting work.

I am thankful to Nokia for using their LTE test network, Anite Finland for providing field measurement software, Nemo Outdoor and Nemo Analyzer, and Elisa for providing LTE data card that is used in the measurements.

Last but not the least, I would like thank my friends and family for their moral support, love and encouragement.

This thesis is dedicated to my parents for their unconditional love.

Tampere, Finland
November 2014

Jay Kant Chaudhary
jaykant2063@gmail.com

TABLE OF CONTENTS

LIST OF ABBREVIATIONS

1G	First Generation
2G	Second Generation
3G	Third Generation
4G	Fourth Generation
5G	Fifth Generation
3GPP	Third Generation Partnership Project
A/D	Analog-to-Digital
ADSL	Asymmetric Digital Subscriber Line
AMPS	Advanced Mobile Phone System
AN	Access Network
AuC	Authentication Centre
BBERF	Bearer Binding and Event Report Function
BS	Base Station
BSC	Base Station Controller
CDF	Cumulative Distribution Function
CN	Core Network
CP	Cyclic Prefix
D/A	Digital-to-Analog
DAB	Digital Audio Broadband
D-AMPS	Digital Advanced Mobile Phone System
DFT	Discrete Fourier Transform
DL	Downlink
DS-CDMA	Direct Sequence Code Division Multiple Access
DVB	Digital Video Broadband
ECN	Evolved Core Network
EDGE	Enhanced Data Rates for GSM Evolution
eNodeB	E-UTRAN NodeB
EPC	Evolved Packet Core
EPS	Evolved Packet System
E-UTRAN	Evolved Universal Terrestrial Radio Access Network
ETSI	European Telecommunications Standard Institute
FDD	Frequency Division Duplex
FFT	Fast Fourier Transform
GGSN	Gateway GPRS Support Node
GPRS	General Packet Radio Service
GSM	Global System for Mobile Communications
HLR	Home Location Register
HPBW	Half-Power Beamwidth
HSDPA	High-Speed Downlink Packet Access

HSPA	High-Speed Packet Access
HSS	Home Subscriber Service
IDFT	Inverse Discrete Fourier Transform
IFFT	Inverse Fast Fourier Transform
IMS	IP Multimedia Subsystem
IMT-A	International Mobile Telecommunications-Advanced
IOs	Interfering Objects
IP	Internet Protocol
ISDN	Integrated Services Digital Network
ISI	Inter-Symbol Interference
ITU-R	International Telecommunication Union-Radiocommunications
J-TACS	Japanese Total Access Communications System
LoS	Line-of-Sight
LTE	Long-Term Evolution
LTE-A	LTE-Advanced
Max	Maximum
ME	Mobile Equipment
MIMO	Multiple Input Multiple Output
Min	Minimum
MM	Mobility Management
MME	Mobile Management Entity
MPC	Multipath Component
MPG	Mobile Performance Gaming
MS	Mobile Station
NAS	Non-Access Stratum
NMT	Nordic Mobile telephone
NTT	Nippon Telegraph and Telephone
OFDMA	Orthogonal Frequency Division Multiple Access
OFDM	Orthogonal Frequency Division Multiplexing
PA	Power Amplifier
PAPR	Peak-to-Average Power Ratio
PCC	Policy and Charging Control
PCRF	Policy and Charging Rules Function
P-GW(or PDN-GW)	Packet Data Network Gateway
PDN	Packet Data Network
PLC	Power Line Communication
P/S	Paraller-to-Serial
PSTN	Public Switch Telephone Network
QAM	Quadrature Amplitude Modulation
QoS	Quality of Service
QPSK	Quadrature Phase Shift Keying
RF	Radio Frequency

RMS	Root Mean Square
RNC	Radio Network Controller
RRH	Remote Radio Head
RRM	Radio Resource Management
RSRP	Reference Signal Received Power
RSRQ	Reference Signal Received Quality
RSSI	Received Signal Strength Indicator
RX	Receiver
SAE	System Architecture Evolution
SAE-GW	System Architecture Evolution Gateway
s.d.	Standard Deviation
SC-FDMA	Single Carrier Frequency Division Multiple Access
S-GW	Serving Gateway
SIM	Subscriber Identity Module
SINR	Signal-to-Interference-plus-Noise Ratio
SNR	Signal-to-Noise Ratio
SON	Self-Organizing Network
S/P	Serial-to-Parallel
TE	Terminal Equipment
TTI	Transmit Time Interval
TUT	Tampere University of Technology
TX	Transmitter
UE	User Equipment
UISC	Universal Integrated Service Card
UL	Uplink
UMTS	Universal Mobile Telecommunications System
UP	User Plane
USIM	Universal Subscriber Identity Module
VDSL	Very High Bit Rate Digital Subscriber Line
VoIP	Voice over IP
VSWR	Voltage Wave Standing Ratio
WAP	Wireless Application Protocol
WCDMA	Wideband Code Division Multiple Access
WiMAX	Worldwide Interoperability for Microwave Access
WLAN	Wireless Local Area Network
X-pol	Cross Polarization

LIST OF SYMBOLS

γ	Path loss exponent
Δf	Subcarrier spacing
η_1	Refractive index of medium 1
η_2	Refractive index of medium 2
θ_{i}	Angle of incidence
θ_{r}	Angle of reflection
λ	Wavelength of propagating wave
$\overline{\tau}$	Average delay spread
$\overline{\phi}$	Mean angle
a_f	Attenuation factor in decibels per floor
a_w	Attenuation factor in decibels per wall
D	Reuse distance
d_{km}	Distance in km
f	Frequency of propagating wave
f_{m}	Maximum Doppler shift
G_{t}	Transmitting antenna gain
G_{r}	Receiving antenna gain
h_{b}	Height of base station
h_{m}	Height of mobile station
L(dB)	Path loss in dB
L_1	Reference path loss at r = 1 m
L_{wi}	Penetration loss for a wall of type i
L_f	Loss per floor
L_{F}	Free space loss
n_{wi}	Number of walls crossed by direct path of type i
n_f	Number of floors crossed by the path
N	Number of cells per cluster
P_{t}	Transmitted power
$P_\tau(\tau)$	Power delay profile
P_{τ_tot}	Total delay
$P(\phi)$	Angular distribution
P_{ϕ_tot}	Total power

R	Radius of the cell
S_τ	RMS delay spread
T_C	Coherence time
T_u	Per-subcarrier modulation time
W	Number of wall types

LIST OF FIGURES

LIST OF TABLES

1 INTRODUCTION

The telecommunication industry has witnessed a phenomenal growth from the traditional means of communications where people used smoke signal and semaphore to the more recent under development 5G (Fifth Generation) technology. Not only there has been a rapid increase in the number of subscribers but also mobile communication systems have revolutionized the way people communicate.

The evolution of 1G (First Generation) cellular system started with Nippon Telegraph and Telephone (NTT)'s Japanese Total Access Communication System (J-TACS) in 1979 in Japan. 1G system consists of other incompatible systems such as Nordic Mobile telephone (NMT) used in Nordic countries in 1981 and Advanced Mobile Phone System (AMPS) in North America in 1983 [1]. These systems used analog circuit-switched technology with Frequency Division Multiple Access (FDMA) as an air channel multiple access technique and supported only voice communications. 1G systems had a large phone size and were quite unsecure. Moreover, they suffered from poor voice quality and poor battery life. [1]

2G (Second Generation) mobile phone systems emerged in 1990s and were based on digital technology. The most popular 2G wireless technology is Global System for Mobile Communications (GSM) and is standardized by the European Telecommunications Standard Institute (ETSI) in Europe [1]. The GSM system uses Time Division Multiple Access (TDMA) and FDMA. The U.S. utilized Interim Standard 54 (IS-54) and Interim Standard 136 (IS-136) based on TDMA technique. IS-54 and IS-136 are also known as D-AMPS (Digital AMPS). Another 2G system popular in the U.S. was Interim Standard 95 (IS-95), also called cdmaOne, but unlike IS-54 and IS-136, it was based on CDMA technique. [1]

2G systems were mainly circuit-switched and designed to carry voice traffic. Global roaming was possible with 2G systems [1]. 2G wireless technologies can handle limited data capabilities such as fax, SMS services as well as Wireless Application Protocol (WAP) services at the data rate of 9.6 kbps or 14.6 kbps, but it is not suitable for web browsing and multimedia applications [1].The GSM system was upgraded to 2.5G to provide higher data speeds with the introduction of General Packet Radio Service (GPRS) technology. GPRS, which is also known as 2.5G, offers a maximum theoretical speed up to 171.2 kbps when all eight timeslots are utilized at once [2]. Later, Enhanced Data Rates for GSM Evolution (EDGE) extended data services of GSM further up to 384 kbps [2].

Growing needs of higher data led to the development of 3G (Third Generation) mobile networks. It was developed as Universal Mobile Telecommunications System (UMTS) in Europe and CDMA2000 in America. Wideband CDMA (WCDMA) is the

air interface of UMTS. UMTS was standardized by 3GPP (Third Generation Partnership Project) and offers speed up to 144 kbps, 384 kbps and 2 Mbps for moving vehicles, pedestrian users and stationary users, respectively [3]. 3G systems support additional features such as full motion video, streaming music, 3D gaming, navigation and faster web browsing. Enhancement in 3G systems was realized by the development of High-Speed Packet Downlink Access (HSDPA) in High-Speed Packet Access (HSPA) family which is also known as 3.5G [3].

Long-Term Evolution (LTE) is a complete IP based technology. LTE Release 10, completed in 2012, is a full 4G technology and is explained in detail in Chapter 3.

5G denotes the next major phase of mobile telecommunications standards beyond the current 4G International Mobile Telecommunications-Advanced (IMT-A) standards. Industrial standards and finer details of 5G systems are yet to be decided by telecommunication companies or standardization bodies [4]. South Korea, UK, USA and some European countries like Sweden and Finland have already started a research on it. However, quite recently in a super-fast 5G test, a South Korean company, Samsung Electronics, has been able to achieve a jaw-dropping data speed of 7.5 Gbps (940 MB per second) stationary and uninterrupted 1.2 Gbps (150 MB per second) while travelling at over 100 km/h using a high frequency 28 GHz signal. Although 28 GHz signal has a short range, the Hybrid Adaptive Array Technology was deployed which uses millimeter wave frequency bands to enable the use of higher frequencies over greater distances. [5] Following a 10 year gap trend between each new generation technology, it is expected that 5G deployment will start around 2020.

The use of smartphones or similar devices has significantly increased these days. Currently, users expect a ubiquitous and very high quality service. This thesis is motivated by the following questions:

- Are users aware of how the signal reception is affected by their locations/positions?
- How can the reception be improved?
- Which location would provide optimal solution for a particular indoor environment?

The aim of this thesis is to demonstrate the effects on the received signal power levels and guide users to positions in such a way that could benefit both the users and operators. Staying at a better location, the users could reduce unwanted radiation, increase the battery lives and they would have better download and upload speeds. On the other hand, operators will benefit from the reduced cost and increased capacity due to less radio energy consumption at the Base Stations (BSs) and Mobile Stations (MSs).

2 WIRELESS COMMUNICATION PRINCIPLES

In the last decades, the wireless communication systems have been widespread all over the world. They involve the exchange of information between two points without any physical connection. The information propagates in the form of electromagnetic waves through air. Different kinds of wireless communication systems such as Bluetooth, Infrared, Wireless Local Area Networks (WLANs), Cordless systems, Paging systems, and Cellular Communication systems are commonly used means of communication. In this chapter, the cellular communications system, radio propagation mechanisms, propagation environments, factors affecting radio propagation and propagation models are explained.

2.1 Cellular Concept

The early mobile radio systems used a single high powered transmitter (TX) with an antenna mounted on a tall tower to cover a single geographical area. However, with the increase in the demands of higher capacity, it was realized that it was almost impossible to reuse those same frequencies throughout the system [6]. The cellular concept was developed at the Bell Laboratories in the 1960s and 1970s.

As the demands of the users for higher capacity and higher data rates increased, a need of new concept was realized which could solve the spectral congestion problem and at the same time also provide users higher capacity and higher data rates. This led to the development of the cellular concept.

The main reason behind the cellular concept are channels that can be time, frequency and/or code words, which are scarce resources and must be used by the operators and network planners as efficiently as possible. By dividing a larger area into smaller cells, the same channels could be utilized more frequently.

A radio transmitter will have only a certain coverage area and the signal level will reach a minimum threshold level at the cell edge below which it cannot be used and will not cause significant interference to the other radio transmitter. This means that it is possible to reuse a channel outside the range of the transmitter. Thus, it is possible to split up an area into several smaller regions, each covered by a different transceiver station. This is called the cellular concept. A portion of the total number of the available channels is allocated to each base station and the neighbouring base stations are assigned different groups of channels so that interference between base stations is minimized [6]. The cells using the same set of frequency channels are known as co-channels cells.

Theoretically, the shape of a cell can be circular, square or hexagonal and is chosen in such a way that it is geometrical, cover the areas without an overlap or no gaps and has the largest possible area. Hence, the possible cell shape choices are: a square, an

equilateral triangle and a hexagon [6]. Hexagonal cell shape is simplistic, conceptual and universally accepted model. However, in reality cells have irregular boundaries because of the terrain over which they travel. Based on the coverage and capacity requirements, different cell types such as macro cells, micro cells or pico cells are employed.

Figure 2.1 illustrates a frequency reuse concept with a cluster size of 3. The cells labelled with the same colour use the same group channels and are co-channel cells. These co-channels are separated by a minimum distance, known as a reuse distance *D*, and is given by [6]

$$D = R\sqrt{3N}, \tag{2.1}$$

where *R* is the radius of the cell and *N* is number of cells per cluster. It can only have values which satisfy Equation (2.2)

$$N = i^2 + ij + j^2, \tag{2.2}$$

where *i* and *j* are non-negative integers. Possible values of *N* are for example 1, 3, 4, 7, 9, 12, 13, 15, 17, 19 [6].

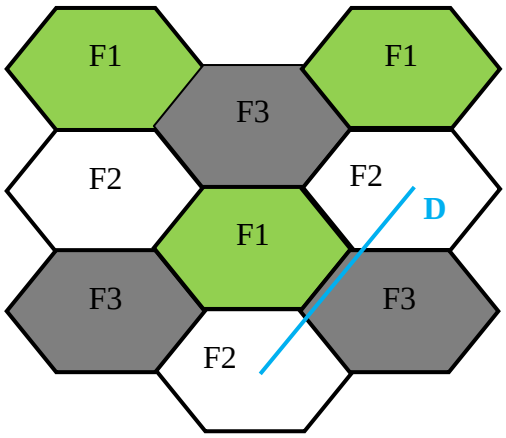

Figure 2.1. *Hexagonal cell frequency reuse factor of 3.*

Many advantages in cellular concept are noted compared to traditional systems that used single transmitter to cover a single whole geographical area, such as lower power consumption, better battery life and more capacity. As the height of the transmitter decreases, the cell sizes become smaller and the smaller cells require less power consumption. This helps to reduce mobile battery consumption. On the other hand, there are some disadvantages as well. More base stations are needed to cover one large area with smaller cells and this increases the overall constructional cost. In addition, seamless handoffs also need to be ensured between the cells.

2.2 Radio Propagation Environment

The radio propagation and hence coverage and capacity largely depend on the environment on which it propagates. It affects the performance of the system. The radio environment can be categorized as shown in Figure 2.2 [7].

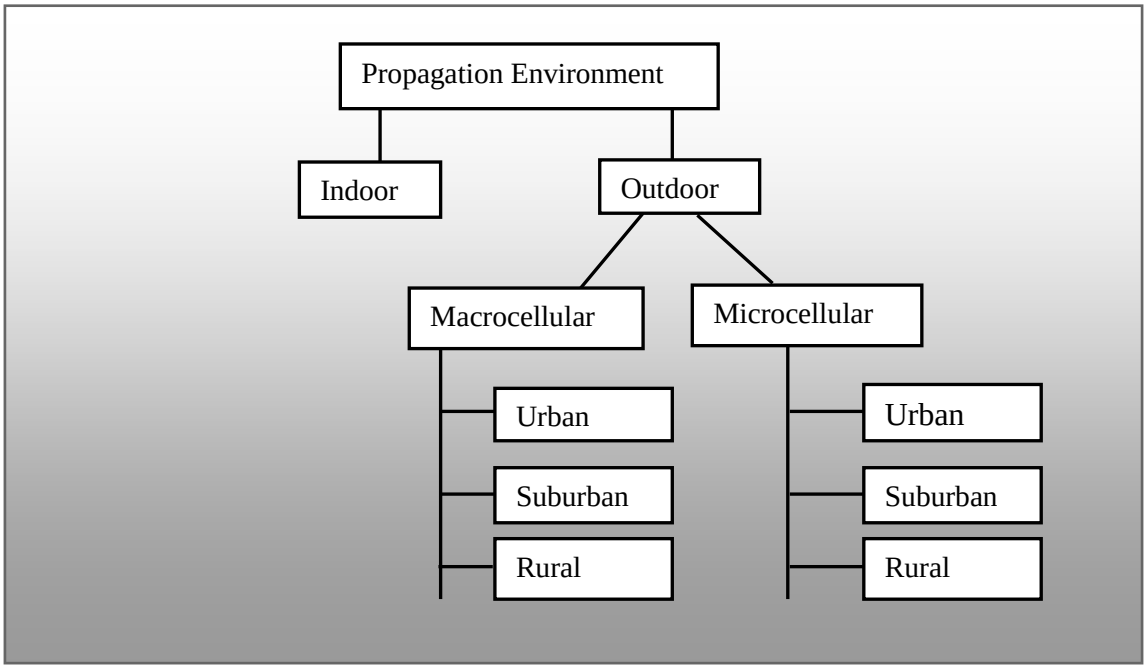

Figure 2.2. *Classification of radio propagation environments.*

- **Mobile terminal location:** The mobile terminal can be either inside or outside. If the mobile terminal is located inside the building, propagation environment is called indoor, otherwise it is called outdoor.
- **Antenna location:** Depending upon the location of the antenna, the environment can be macrocellular, microcellular or picocellular. In macrocellular, the antenna height is above the average height of the building whereas in microcellular, the antenna height is below the average height of the buildings. Pico cells are smaller cells than macro and micro cells, and are used to cover very small areas such as particular areas of buildings or possibly tunnels where coverage from a larger cell is not possible [7].
- **Morphology type:** Depending upon the variation of the size and density of both the man- made and natural obstacles, the environment can be urban, suburban or rural [7]. Urban areas, such as cities or towns, have high population with buildings higher than three or four floors. The microcellular environments usually exist in urban areas. The rural area has the least population density and generally located far from the city. Typically rural area has macrocellular environment. The suburban area has population density higher than rural area but lesser than urban area. These are normally a part of big cities or towns. [7]

2.3 Radio Propagation Mechanisms

A signal propagates in the form of electromagnetic waves in free space. A part of the electromagnetic energy radiated by the antenna of the transmitting station reaches to the receiving station through different paths and is exposed to a variety of man-made structures and different terrain types [8]. Along these paths, various interactions occur between the electromagnetic fields and objects. The possible interactions are reflection, transmission, diffraction and scattering. Because of these interactions, there are variations in the signal power levels and hence in the coverage and quality of the networks.

2.3.1 Free Space Propagation

The free space propagation model is used to predict the received signal strength when the transmitter and the receiver (RX) has a clear, unobstructed line-of-sight (LoS) path between them. Generally, this model is used for satellite communication and in microwave LoS radio links. The received power at a distance *d* from the transmitting antenna is given by the Friis free space equation [6]

$$P_{\mathrm{r}}(d) = \frac{P_{\mathrm{t}} G_{\mathrm{t}} G_{\mathrm{r}}}{\left(\frac{4\pi d}{\lambda}\right)^2}, \tag{2.3}$$

where P_{t} is transmitted power, G_{t} is transmitting antenna gain, G_{r} is receiving antenna gain and λ is the wavelength of propagating wave.
Equation (2.3) can be simplified to find the path loss *L* in dB as

$$L(\mathrm{dB}) = 32.4 + 20\log d_{\mathrm{km}} + 20\log f_{\mathrm{MHz}}, \tag{2.4}$$

where f_{MHz} is the frequency of the propagating wave in MHz and d_{km} is the distance between the TX and the RX in km.

2.3.2 Reflection and Transmission

Reflection occurs when a propagating electromagnetic wave impinges on an object which has very large dimensions compared to the wavelength of the propagating wave. When a wave propagates from a medium to another medium having different electrical properties, a part of the wave is reflected back to the original medium, known as the reflected wave and a part of the wave is transmitted (refracted) to the second medium known as the refracted wave. If the second medium is a perfect conductor, then all the incident energy is reflected back to the first medium without a loss of energy. For indoor propagation, transmission of radio waves is essential because BSs are located

either outside or inside the buildings and the transmitted radio waves need to penetrate through walls and floors before reaching to the RX. Reflection and refraction can occur from the surface of earth, buildings or walls.

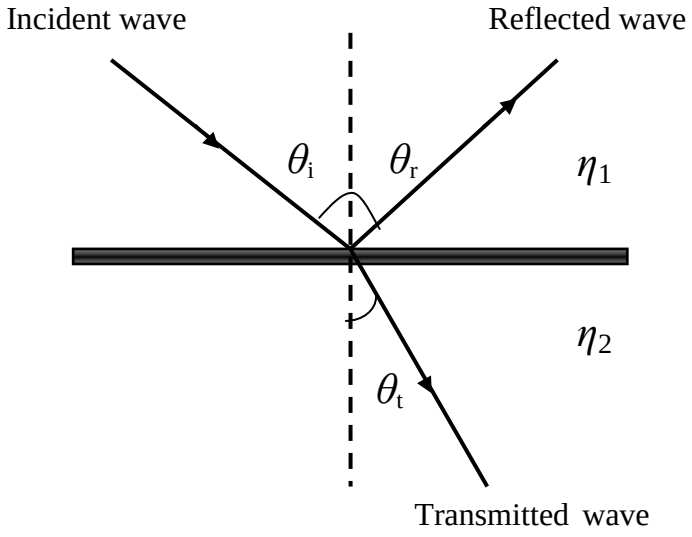

Figure 2.3. *Reflection and transmission of a wave.*

For reflection and transmission shown in Figure 2.3, Snell's law of reflection and Snell's law of refraction are obeyed and are defined in Equations (2.5) and (2.6) [9].

Snell's law of reflection:

$$\theta_i = \theta_r \tag{2.5}$$

Snell's law of refraction:

$$\frac{sin\theta_i}{sin\theta_t} = \frac{\eta_2}{\eta_1}, \tag{2.6}$$

where θ_i is the angle of incidence, θ_r is the angle of reflection and θ_t is the angle of refraction. η_1 and η_2 are the refractive indices of the first and second medium respectively.

2.3.3 Diffraction and Scattering

Diffraction occurs when a wave encounters sharp irregularities, obstacles or slits. Diffraction causes bending of an incident wave around a corner as shown in Figure 2.4 (a). The effects due to diffraction are more pronounced when the wavelengths of the incident wave are roughly comparable to the dimensions of the diffracting object or slit. The phenomenon of diffraction can be explained by Huygen's principle, which states

that every point on a wavefront can be considered as a source of secondary wavelets and that these wavelets combine to produce a new wavefront in the direction of propagation [6].

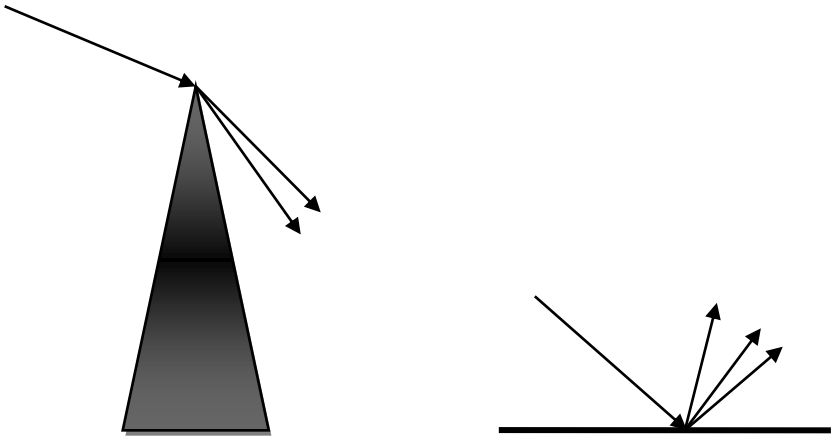

(a) (b)

Figure 2.4. *Diffraction and scattering a wave.*

Scattering occurs when a wave propagates through a medium having objects whose dimensions are smaller than the wavelength of the propagating wave. Equation (2.5) is applicable in case of a specular reflection where the surfaces are smooth. However, in practice, the surfaces are rough and when the wave impinges on such rough surfaces, the wave is scattered into different directions as shown in Figure 2.4 (b). The degree of scattering depends on the angle of incidence and on the roughness of the surface in comparison to the wavelength [9].

2.4 Multipath Propagation

For wireless communication, the transmission medium is the radio channel between the transmitter and the receiver. The signal can get from the TX to the RX via a number of different propagation paths as shown in Figure 2.5. [10] The propagation may occur by the direct LoS between the TX and the RX or by reflection, diffraction or scattering from the interfering objects. Thus, the transmitted signal may undergo multiple reflections refractions, diffractions and scatterings, due to which the signal is received from multiple paths at different time instants. This is known as multipath propagation. Each multipath component (MPC) will have different amplitudes, phases and angles of arrivals. These MPCs are combined at the receiver antenna which may be either constructive or destructive depending upon the phases of MPCs. When MPCs are not in same phase they interfere with each other.

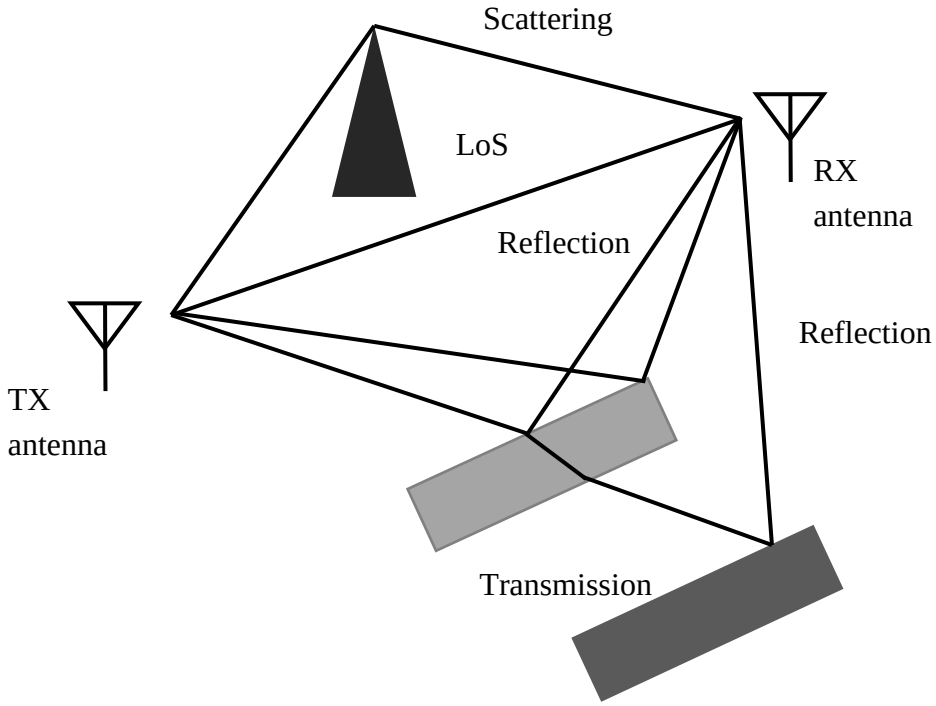

Figure 2.5. *Multipath propagation.*

2.4.1 Delay Spread

In multipath propagation, the replicas of the transmitted signal are received from different paths at different time instants. The time differences of these multipath components are defined by a delay spread. It is the time delay between the arrival of the first signal component (LoS or multipath) and the last received signal component. The rms delay spread S_τ of the multipath components is calculated from power delay profile $P_\tau(\tau)$ and is given by [11]

$$S_\tau = \sqrt{\frac{\int_0^\infty (\tau - \bar{\tau})^2 P_\tau(\tau) d\tau}{P_{\tau\_\text{tot}}}} \tag{2.7}$$

where $\bar{\tau}$ is average delay spread and P_{τ_tot} is total delay. Equations (2.8) and (2.9) are used to calculate average delay spread and total delay [11].

$$\bar{\tau} = \sqrt{\frac{\int_0^\infty \tau P_\tau(\tau) d\tau}{P_{\tau\_\text{tot}}}}\,. \tag{2.8}$$

$$P_{\tau\_\mathrm{tot}} = \int_0^{\infty} P_\tau(\tau) d\tau \,. \tag{2.9}$$

Coherence time T_C is the time domain equivalent of the Doppler spread and gives the statistical measure of the time duration over which the channel response is essentially constant. If the coherence time is defined for 50 % of the time correlation function then the coherence time is approximated by [6]

$$T_C \approx \frac{9}{16\pi f_\mathrm{m}}, \tag{2.10}$$

where f_m is the maximum Doppler shift given by $f_\mathrm{m} = \frac{v}{\lambda}$.

In order to understand the effects off the delay spread, it needs to be compared it with the coherence time. If the delay spread is small compared to the coherence time, then time spreading in the received signal is little. However, when the delay spread is relatively large, time spreading of the received signal is significant which can lead to substantial signal distortion [11].

2.4.2 Angular Spread

Angular spread describes the deviation of signal incident angle. It is calculated in both horizontal and vertical planes using the formula [7]

$$S_\phi = \sqrt{\int_{\bar{\phi}-180}^{\bar{\phi}+180} \left(\phi - \bar{\phi}\right)^2 \frac{P(\phi)}{P_{\phi\_\mathrm{tot}}} d\phi}, \tag{2.11}$$

where $\bar{\phi}$ is the mean angle, $P(\phi)$ is the angular distribution and P_{ϕ_tot} is the total power. Angular spread is used to define the environment type and its value is different for different environment types. Its value is 5–10 degrees in macro cells and 45 degrees in micro cells. In indoor cells, the incoming signal witnesses deviation from different directions and hence its value can be even higher, up to 360 degrees [7].

2.4.3 Coherence Bandwidth

Coherence bandwidth is a measure of the maximum frequency difference for which signals are strongly correlated in amplitude for different frequencies [6]. In other words, it is a measure of range of frequencies over which the frequency response of the channel is constant. When the frequency response of the channel is constant, it allows to pass all

the spectral components of the signal with approximately equal gain and linear phase. Coherence bandwidth Δf_c is related to the delay spread S_τ as [7]

$$\Delta f_c = \frac{1}{2\pi S_\tau}. \tag{2.12}$$

A system may be wideband or narrowband depending on the coherence bandwidth. If the system bandwidth is higher than the coherence bandwidth of the channel, it is called a wideband system. In this case, there will be more distortion in the signal. On the other hand, if the system bandwidth is less than the coherence bandwidth of the channel, then the system is said to be a narrowband system where the amplitudes of the signal will change rapidly, but the signal will not be distorted in time. [6]

2.5 Fading of Radio Waves

The transmitted wave reaches the receiver from multiple paths at different time instants with different amplitude, phase and angle of arrival. These multipath components interfere with each other when they are not in same phase. The amplitude of the total signal changes if TX, RX or Interfering Objects (IOs) are moving. This effect of changing the total signal amplitude due to interference of the different MPCs is called small-scale fading or simply fading. A channel may be slow fading channel or fast fading channel based on coherence time and symbol period, and flat fading channel or frequency selective fading channel based on coherence bandwidth and signal bandwidth [6].

2.5.1 Slow Fading

In slow fading channel, the channel impulse response changes at a rate much slower than transmitted baseband signal [6]. In other words, a signal undergoes slow fading if the symbol duration is much smaller than the coherence time. Slow fading occurs when there are obstacles such as buildings, mountains or hills in between the base station and mobile station. These obstacles shadow the signal. Slow fading is therefore also called shadowing. There exits variations in the local mean value of the signal over a wider area and these variations are log-normally distributed. Hence, slow fading is also called log-normal fading [7]. Slow fading margin is used to minimize the effects of slow fading.

2.5.2 Fast Fading

Fast fading is caused by multipath propagation and the movement of the TX, RX and/or environment. In a fast fading channel, the channel impulse response changes rapidly compared to the transmitted baseband signal. In other words, a signal undergoes fast fading if symbol period is larger than the coherence time of the channel.

2.5.3 Flat Fading

Flat fading channels are also known as narrowband channels. For flat fading, the coherence bandwidth of the channel is greater than the bandwidth of the transmitted signal. Therefore, all frequency components of the signal will experience the same magnitude of fading.

2.5.4 Frequency Selective Fading

For frequency selective fading, bandwidth of the spectrum of the transmitted signal is greater than the coherence bandwidth of the channel. For this reason, frequency selective fading channels are also known as wideband channels. Frequency selective channels are much more difficult to model than flat fading channels [6].

2.5.5 Propagation Slope

A Propagation slope describes how the radio wave is attenuating over a distance and is expressed in dB/decade. The propagation slope is defined by the propagation exponent γ, (also called path loss exponent) which depends on the environment type. For example, in free space the propagation exponent is 2 and this corresponds to a propagation slope of 20dB/decade. The propagation slope can be calculated from the propagation exponent using [7]

$$L = L_0 d^{(\gamma/10)}. \tag{2.13}$$

A propagation slope at close to the BS follows the inverse square law. Therefore, the propagation slope near the transmitting antenna is lower compared to that at greater distances. The distance of propagation slope change is called the breakpoint distance B and is calculated by Equation (2.14)

$$B = 4\frac{h_b h_m}{\lambda}, \tag{2.14}$$

where h_b and h_m are the heights of the base station and the mobile station, respectively.

2.6 Propagation Models

Propagation models are used to find the maximum allowable path loss between a transmitter and a receiver and based on this value, the coverage range can be calculated. The common propagation models are: empirical models, physical or semi-empirical models, deterministic models and indoor models.

2.6.1 Empirical Models

Empirical models are typically represented by mathematical equations derived from extensive measurement using regression methods. These models are mainly suited for macrocellular environments and more accurate in the environments with same characteristics. However, these can be used in other environments as well with appropriate fine tuning. These models are simple, easy to use and require less computational time. However, these methods do not take into account physical propagation mechanisms such as reflection and diffraction, which is one of the biggest drawbacks.

Okumura-Hata Model

The initial model was given by Okumura based on the series of extensive measurements taken in Tokyo city and was later well formulated by Hata based on these data [12]. Okumura-Hata model is one of the mostly used methods and is often used as a standard to compare with other methods. This model is particularly suited for macrocells. In Okumura-Hata model, the prediction area is divided into three categories: open, suburban and urban areas. Urban area is further sub-divided into large cities and medium-small cities, where an area having an average building height above 15 m is defined as a large city [9]. This model can be expressed as [9]

$$\begin{aligned} &\text{Urban areas:} && L_{dB} = A + B\log R - E \\ &\text{Suburban areas:} && L_{dB} = A + B\log R - C \\ &\text{Open areas:} && L_{dB} = A + B\log R - D, \end{aligned} \tag{2.15}$$

where the parameters *A, B, C, D* and *E* are defined as

$$\begin{aligned} A &= 69.55 + 26.16\log f_c - 13.82\log h_b \\ B &= 44.9 - 6.55\log h_b \\ C &= 2(\log(f_c / 28))^2 + 5.4 \\ D &= 4.78(\log f_c)^2 - 18.33\log f_c + 40.94 \\ E &= 3.2(\log(11.75h_m))^2 - 4.97 \text{ for large cities, } f_c \geq 300 \text{ MHz} \\ E &= 8.29(\log(1.54h_m))^2 - 1.1 \text{ for large cities, } f_c < 300 \text{ MHz} \\ E &= (1.1\log f_c - 0.7)h_m - (1.56\log f_c - 0.8) \text{ for medium to small cities.} \end{aligned} \tag{2.16}$$

Table 2.1. *Parameters of Okumura-Hata model and their range.*

Parameter	Range
Frequency (f_c)	150–1500 MHz
BS height (h_b)	30–200 m
MS height (h_m)	1–10 m
Range (R)	> 1 km

Table 2.1 shows that Okumura-Hata model is valid only for 150 MHz $\leq f_c \leq$ 1500 MHz, 30 m $\leq h_b \leq$ 200 m, 1m < h_m < 10 m and R > 1 km.

COST-231 Hata Model

In order to extend the frequency range, Okumura-Hata model for medium to small cities was modified which gave a new model called COST-231 Hata model [13]. In this model, range is extended from 1500 MHz to 2000 MHz. and path loss is calculated using [9]

$$L_{dB} = F + B\log R - E + G, \tag{2.17}$$

where

$$F = \begin{cases} 69.55 + 26.16\log f_c - 13.82h_b \text{ for } 150 \text{ MHz} \leq f_c \leq 1500 \text{ MHz} \\ 46.3 + 33.9\log f_c - 13.82h_b \text{ for } 1500 \text{ MHz} < f_c < 2000\ MHz \end{cases} \tag{2.18}$$

$$G = \begin{cases} 0 \text{ dB for medium sized cities and suburban areas} \\ 3 \text{ dB for metropolitan areas} \end{cases} \tag{2.19}$$

and E is defined as in equation (2.16).

Table 2.2. *Parameters of COST-231 Hata model and their range.*

Parameter	Value
Frequency (f_c)	150–2000 MHz
BS height (h_b)	30–200 m
MS height (h_m)	1–10 m
Range (R)	1–20 km

Table 2.2 shows that COST-231 Hata model is valid for 150 MHz ≤ f_c ≤ 2000 MHz, 30 m ≤ h_b ≤ 200 m, 1m < h_m < 10 m and 1 km < R < 20 km, where h_b and h_m are the heights of the base station and the mobile station respectively and *R* is the distance between the base station and the mobile station. It also depicts that the COST-231 Hata model can be utilized for higher range of coverage and at higher frequency compared to the Okumura-Hata model.

2.6.2 Physical or Semi-Empirical Models

Physical models take into consideration propagation mechanisms such as diffraction and are mainly suitable for small macrocells or microcells. Physical models are more accurate than empirical models but require more precise description on environments than empirical ones and more computational time. One popular method for this model is the COST-231-Walfisch-Ikegami model [10].

2.6.3 Deterministic Models

Deterministic models give analytical estimations of radio waves. Basically, these models can predict all kinds of propagation phenomena such as transmission, diffraction, scattering and attenuation. These models require very detailed and accurate input parameters such as material parameters and 3D building information. They produce quite accurate results but require extensive computational time.

2.6.4 Indoor Models

Indoor radio propagation has drawn lot of interest these days. Like outdoor, the indoor models are dominated by same mechanisms like reflection, diffraction and scattering. However, the variability of the environment is much greater. For example, propagation within buildings is strongly affected by features such as layout of the building, the construction material, and the building type. [6] Indoor differs from outdoor (macro/micro) due to shorter distances.

2.6.5 Indoor Empirical Models

In this section, Wall and Floor Factor model, International Telecommunication Union-Radiocommunications (ITU-R) model, COST-231 Multi-Wall and Ericsson model model are discussed.

Wall and Floor Factor Model

This model is an extension to a simple path loss model introduced by Keenan, who characterizes indoor path loss exponent with 2, just as in case of free space, and introduces two additional attenuation parameters related to number of floors n_f and

walls n_w intersected by the straight-line distance r between the terminals. The propagation loss is given as [9]:

$$L = L_1 + 20\log r + n_f a_f + n_w a_w, \tag{2.18}$$

where a_f and a_w are the attenuation factors in decibels per floor and per wall, respectively. L_1 is the reference path loss at r = 1 m.

ITU-R Model

A similar but rather more advance approach is taken by ITU-R model by considering frequency effect and changing the path loss exponent. The path loss exponent n varies depending on the properties of the buildings and the signal frequency. The path loss in dB is given by [9]:

$$L_{\mathrm{T}} = 20\log f_{\mathrm{c}} + 10n\log r + L_f(n_f) - 28, \tag{2.19}$$

where f_c is the frequency of the signal.

COST-231 Multi-Wall Model

This model incorporates a linear component of loss which is proportional to number of walls and floors penetrated and loss is given by [9]:

$$L_{\mathrm{T}} = L_{\mathrm{F}} + L_{\mathrm{c}} + \sum_{i=1}^{W} L_{\mathrm{w}i} n_{\mathrm{w}i} + L_{\mathrm{f}} n_{\mathrm{f}}^{((n_{\mathrm{f}}+2)/(n_{\mathrm{f}}+2)-b)} \tag{2.20}$$

where L_F is the free space loss for LoS path between the transmitter and the receiver, n_{wi} is the number of walls crossed by the direct path of type i, W is the number of wall types, L_{wi} is the penetration loss for a wall of type i. n_f is number of floors crossed by the path, b and L_c are empirically derived constants and L_f is the loss per floor.

The penetration loss L_w depends on frequency and types of wall. For example, its value at 1800 MHz is 3.4 dB and 6.9 dB for light walls and heavy walls, respectively. The floor loss per floor, that is, the last term in Equation 2.20 is shown in Figure 2.6. It depicts that the additional loss per floor decreases with the increasing number of floors [9].

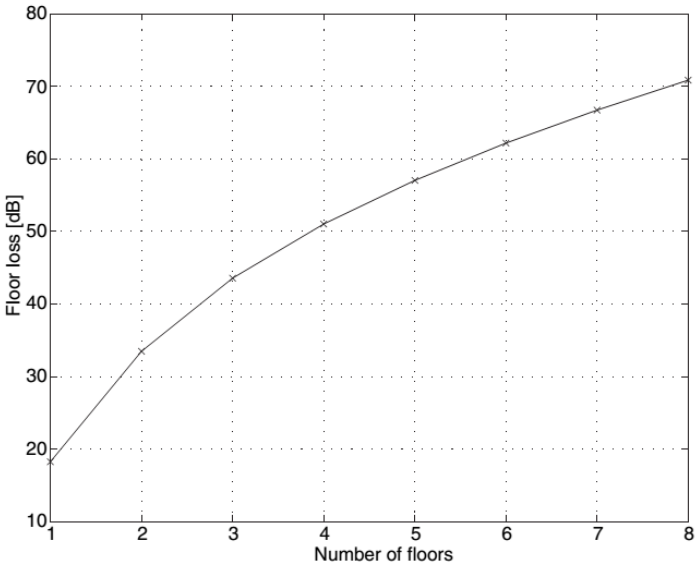

Figure 2.6. *Floor loss for COST-231 multi-wall model [9].*

Ericsson Model

Ericsson model considers the path loss including shadowing as a random variable uniformly distributed between limits which vary with distance as shown in Table 2.3. The path loss exponent increases from 2 to 12 as the distance increases which indicates a very rapid decrease of signal strength with distance. Ericsson model is intended for use around 900 MHz. However, this model can be extended for use at 1800 MHz by adding 8.5 dB extra path loss at all distances. [9]

Table 2.3. *Ericsson indoor propagation model [9].*

Distance [m]	**Lower limit of path loss [dB]**	**Upper limit of path loss [dB]**
$1 < r < 10$	$30 + 20 \log r$	$30 + 40 \log r$
$10 \leq r < 20$	$20 + 30 \log r$	$40 + 30 \log r$
$20 \leq r < 40$	$-19 + 60 \log r$	$1 + 60 \log r$
$40 \leq r$	$-115 + 120 \log r$	$-95 + 120 \log r$

2.6.6 Indoor Physical Models

The indoor propagation physical models use ray tracing and geometrical theory of diffraction. It requires a detailed knowledge of building geometry and materials available. Therefore, these models are more complex and require more time for computation.

3 LTE INTRODUCTION

The number of mobile subscribers has increased tremendously in recent years. At the same time, the demand of higher data rates and quality services has become essential in any network. GSM network was primarily targeted for voice communication and cannot provide high data rates. 3GPP which was started in 1998 introduced UMTS Release 99 in 1999 as the first release of UMTS standard [14]. UMTS combines properties of circuit-switched voice network such as GSM with the properties of the packet-switched data networks such as GPRS and EDGE [15]. However, these systems are still legacy and a new technology called LTE was introduced in 2004 with the aim of providing higher data rates, better quality of service and faster connection.

Table 3.1. *LTE Release 8 major parameters [16].*

Parameter	Values
DL Access Scheme	OFDMA
UL Access Scheme	SC-FDMA
Bandwidth	1.4, 3, 5, 10, 15 and 20 MHz
Modulation	QPSK, 16-QAM, 64-QAM
Subcarrier spacing	15 kHz
Minimum TTI	1 ms
Cyclic prefix short	4.7 μs
Cyclic prefix long	16.7 μs
Spatial multiplexing	Single layer for UL per UE, up to four layers for DL per UE, MIMO support for UL and DL

LTE standardization is being carried out in the 3GPP. LTE Release 8 was finalized in the early 2009 and is considered as 3.9G (near 4G) network. Later releases like Release 9 and Release 10 are more targeted towards LTE-Advanced (LTE-A), which is considered to be a true 4G network. LTE networks provide high peak data rates, improved coverage and capacity, low latency, multiple antenna support, reduced operational cost and seamless connectivity with existing systems such as GSM, UMTS, and HSPA. Table 3.1 shows the major parameters of LTE Release 8 [16]. A LTE network can deliver data rate up to 300 Mbps in Downlink (DL) and 75 Mbps in Uplink (UL) in a 20 MHz system bandwidth with 4 × 4 Multiple Input Multiple Output

(MIMO) technology [17]. This chapter explains LTE architecture, multiple access techniques, MIMO technology and LTE frame structure.

3.1 LTE Architecture

Figure 3.1 shows basic architecture of a LTE network. This architecture can be divided into four high level domains: User Equipment (UE), Evolved Universal Terrestrial Radio Access Network (E-UTRAN), Evolved Packet Core (EPC), and the services domain [17].

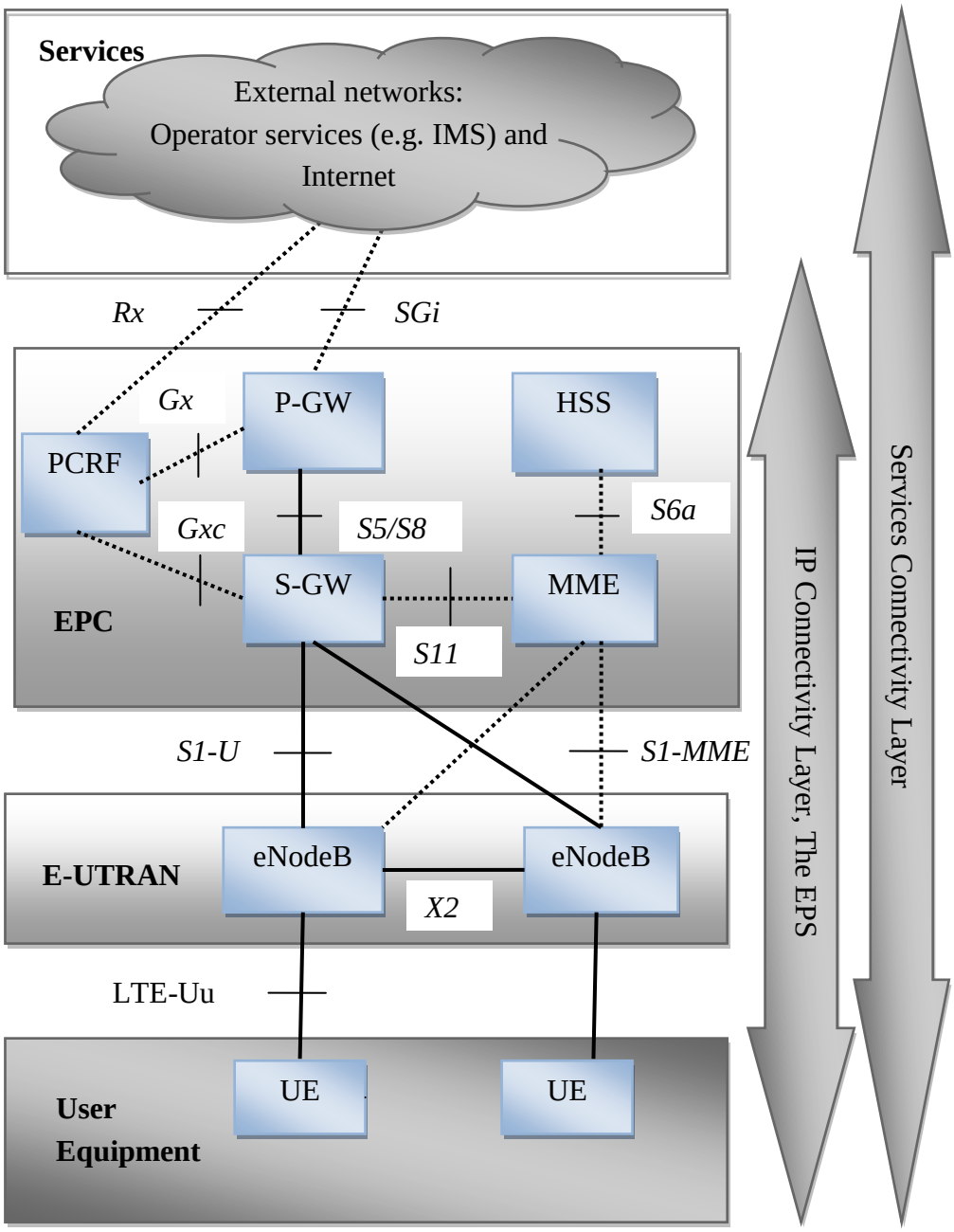

Figure 3.1. *LTE system architecture [17].*

UE, E-UTRAN and EPC together constitute a system called Evolved Packet System (EPS) and they represent Internet Protocol (IP) connectivity layer whose main function is to provide IP based connectivity. All services are offered on top of IP connectivity. It is important to note that the circuit switching nodes and interfaces seen in earlier 3GPP legacy networks are not present in E-UTRAN and EPC. In other words, LTE is a purely packet-switched system.

3.1.1 User Equipment (UE)

The UE is typically a handheld device such as a smartphone or a data card attached to or embedded to a laptop that the end user utilizes for communication. UE contains a Subscriber Identity Module (SIM) known as Universal Subscriber Identity Module (USIM) placed into a removable chip called Universal Integrated Service Card (UISC) [17]. The USIM contains security keys and is used to identify and authenticate the user.

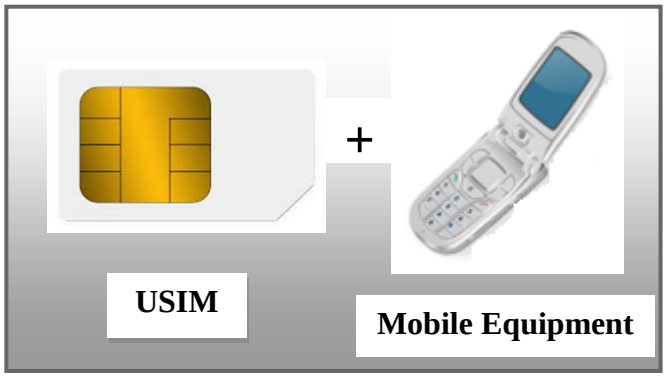

Figure 3.2. *User Equipment.*

Figure 3.2 shows that the UE without a USIM inside it is simply called the Terminal Equipment (TE) or Mobile Equipment (ME). The UE helps in setting up, maintaining and terminating the calls and also provides mobility management functions such as handovers and reporting terminal locations, and is connected to E-UTRAN by the LTE-Uu interface.

3.1.2 E-UTRAN NodeB (eNodeB)

E-UTRAN is typically a collection of Evolved UTRANs from WCDMA network and it consists of eNodeBs. An eNodeB is the LTE equivalent of a UMTS NodeB. eNodeB is the only type of node in the E-UTRAN network and it acts as a layer 2 bridge between UE and EPC [17]. An eNodeB is connected to the neighbouring eNodeBs by means of the X2 interface, to Packet Data Network Gateway (P-GW) of core network by the S1-U interface, and to UEs by means of the LTE-Uu interface.

It is important to note that in LTE there are no nodes between BTS and CN as it used to be Base Station Controller (BSC) in GSM and Radio Network Controller (RNC) in the WCDMA network. The removal of RNC makes the architecture of the network flat and hence requires less time for a packet session, and handover is also easier. Since the

centralized node is removed, eNodeBs are given more functionalities compared to NodeBs. They are responsible for Radio Resource Management (RRM) and Mobility Management (MM). In addition, they also perform ciphering/deciphering of User Plane (UP) data and IP compression/decompression.

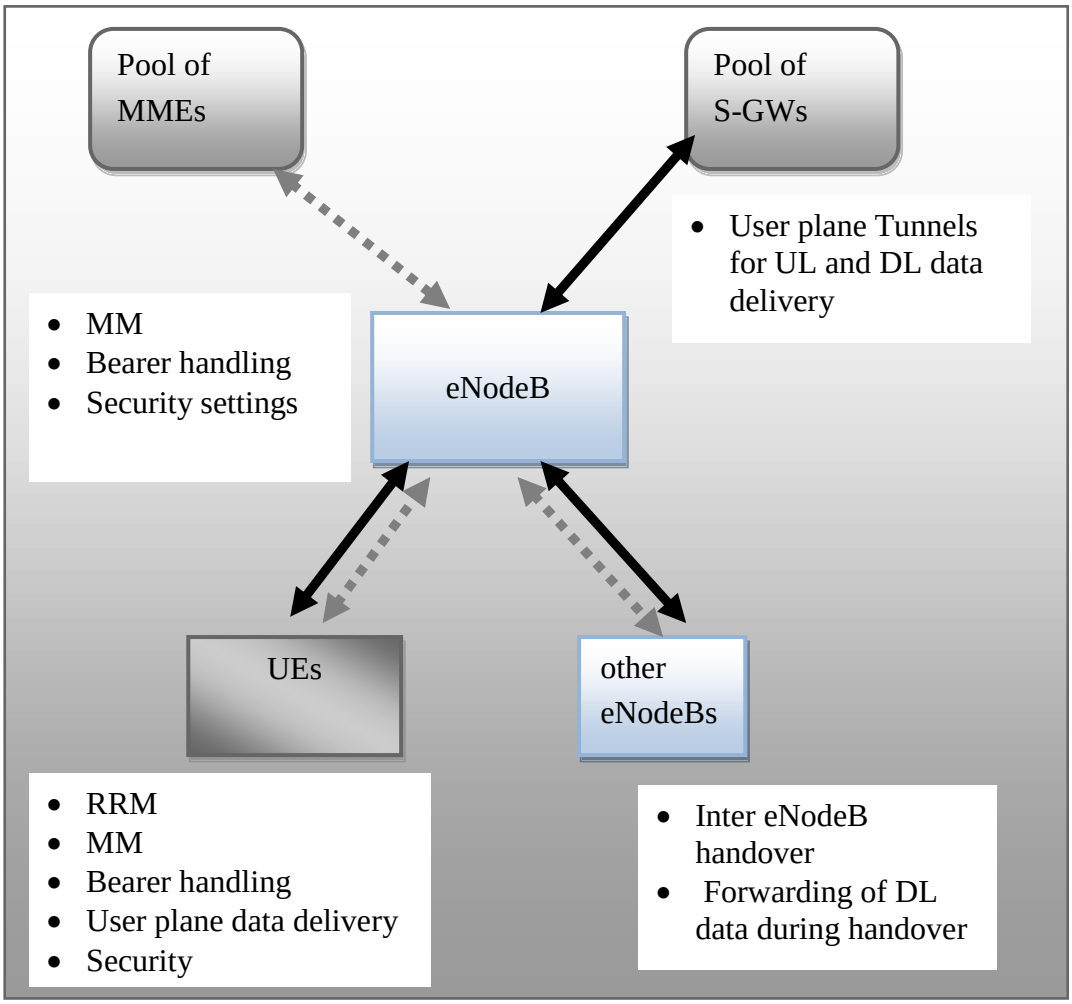

Figure 3.3. *eNodeB connection to other logical nodes and main functions [17].*

Figure 3.3 shows the connections of eNodeB to the surrounding logical nodes and summarizes its main functionalities. eNodeB could have one-to-many or many-to-many relationship with other nodes. One eNodeB may serve multiple UEs, however, a UE is connected to only one eNodeB at a time. LTE network also supports an advance feature called Self-Organizing Network (SON) [17]. SON means a network is able to reconfigure itself and manages the available network resources to achieve the best performance in a cost-effective manner.

3.1.3 Core Network (CN)

There are not only changes in the radio interface but also in the architecture of the core network leading to a new network in System Architecture Evolution (SAE) called Evolved Core Network (ECN). One of the biggest architectural changes is that the EPC

does not contain any circuit-switched domain and there is no direct connectivity to traditional circuit-switched networks such as Public Switch Telephone Network (PSTN) and Integrated Services Digital Network (ISDN) [17]. EPC consists of

- Packet Data Network Gateway (P-GW or PDN-GW)
- Serving Gateway (S-GW)
- Mobile Management Entity (MME)
- Home Subscriber Service (HSS)
- Policy and Charging Rules Function (PCRF)

Control Plane and UP are separated in CN. MME is the control plane entity, and P-GW and S-GW are the UP entity. P-GW and S-GW together are called System Architecture Evolution Gateway (SAE-GW).

P-GW

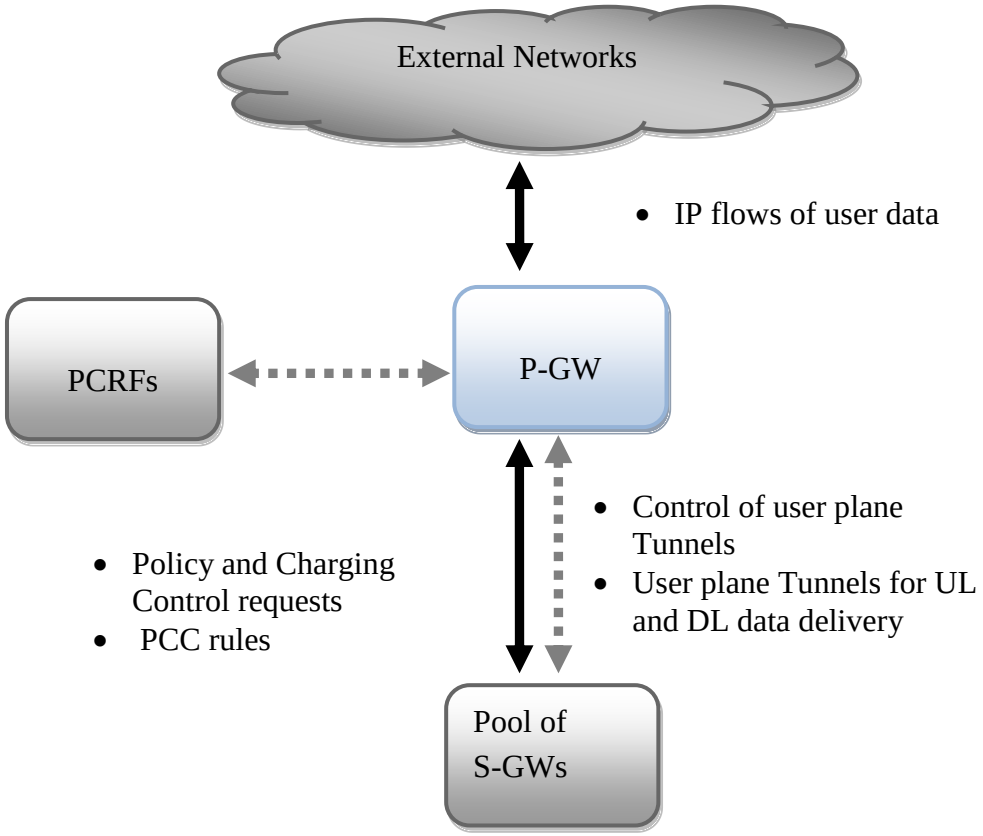

Figure 3.4. *P-GW connections to other logical nodes and main functions [17].*

P-GW, also often abbreviated as PDN-GW, is the anchor router between the EPS and the external packet data networks such as Internet or IP Multimedia Subsystem (IMS). IMS networks provide multimedia services such as Voice over IP (VoIP), video conferencing and messaging [18]. The role of P-GW here is similar to the Gateway GPRS Support Node (GGSN) for GSM/GPRS and WCDMA/HSPA [18]. It is the

highest level mobility anchor in the system [16]. The P-GW usually acts as the IP point of attachment for the UE. IP address is allocated to the UE whenever it wants to communicate with external networks such as the Internet. UE may have simultaneous connectivity to more than one P-GW for accessing multiple packet data networks. Each P-GW may be connected to one or more Policy and Charging Resource Function (PCRF), S-GW and external networks as shown in Figure 3.4. However, for a given UE that is associated with the P-GW, there is only one S-GW [17]. The PCRF performs gating and filtering functions.

S-GW

S-GW is the UP node that connects P-GW of EPC to eNodeB. UP refers to a group of protocols used to support user data transmission throughout the network [18]. The principal functions of S-GW are UP tunnel management and switching. When UE is in the connected mode, it relays data from eNodeB to P-GW and vice versa. When UE is in the idle mode, any packets of data received from P-GW are buffered in S-GW and S-GW requests MME to initiate paging of UE. Paging will cause UE to reconnect and when tunnels are reconnected, the buffered packets will be forwarded to the eNodeB.

UE is connected to only one eNodeB at a time. As UE moves across areas served by different eNodeBs, MME commands the S-GW to switch tunnel from one eNodeB to another to ensure continuous data connection, thus allowing S-GW functioning also as a local mobility anchor. During the time UE makes a handover, MME may also request S-GW to provide tunneling resources for data forwarding. The mobility scenario might also include changing from the old S-GW to a new S-GW [18]. S-GW is connected to eNodeBs via the S1-U interface and to P-GW via the S5-U interface.

MME

MME is the main control element in EPC and operates only in the control plane. It processes signaling between the UE and the CN. The protocols running between the UE and the CN are known as Non-Access Stratum (NAS) protocols. MME is responsible for mobility management, authentication and security, and managing subscription profile and service connectivity. MME and S-GW are connected with the S11 interface which is used by MME to control S-GW. The interface between eNodeB and MME is called the S1-MME and is used to transfer control plane information. MME connects to HSS by means of the S6a interface for the authentication and authorization of users. The S6a interface is an evolution of the Gr interface used by WCDMA/LTE core network to connect to Home Location Register (HLR) [19].

HSS

HSS is a database corresponding to the HLR in the GSM/WCDMA core network that stores subscriber related information [19]. It contains information such as user profile, user location, restrictions on roaming if any, authorization of assigned services and

Packet Data Network (PDN) information. HSS provides a permanent key, which is stored in Authentication Centre (AuC) that is a part of HSS. The Permanent key is used for user authentication to identify right users, and encryption and decryption of user data. In order to support the mobility between a non-3GPP Access Networks (ANs), it also stores information on available P-GWs that a user can connect to. In addition, HSS also holds dynamic information such as the identity of MME into which the user is currently attached or registered [20]. HSS is able to connect with every MME in the whole network, where UEs of MME are allowed to move [17].

PCRF

PCRF is the network element that is responsible for Policy and Charging Control (PCC). It makes decisions on how to handle services in terms of Quality of Service (QoS) and provides information to Policy and Charging Enhancement Function (PCEF) located in P-GW and, if applicable, also to Bearer Binding and Event Report Function (BBERF) located in S-GW [17]. It has mainly two functions – the policy control and the flow-based control [21]. The policy control includes functions such as gating control, QoS control and usage monitoring. The flow-based control on the other hand includes different charging rules such as volume-based, time-based, event-based and different rates based on user characteristics.

3.2 Multiple Access Techniques in LTE

Selection of appropriate modulation and multiple access technique plays an important role to achieve a good system performance. The multiple access technique used in LTE is different from that used in WCDMA. In WCDMA, direct Sequence Code Division Multiple Access (DS-CDMA) is used, whereas LTE uses Orthogonal Frequency Division Multiple Access (OFDMA) in downlink and Single Carrier Frequency Division Multiple Access (SC-FDMA) in uplink [22]. These schemes are described in detail here along with their advantages and motive of using them as transmission schemes.

3.2.1 OFDMA

Unlike single carrier modulation where information is modulated into only one carrier, OFDM is a type of multicarrier modulation where information is divided into many parallel subcarriers and sent over many different subchannels. Each subcarrier is capable of carrying one modulation symbol [9]. Data rate on each of the subchannels is much less than the total data rate, and corresponding subchannel bandwidth is much less than the total system bandwidth [11]. Moreover, bandwidth of each subchannel is less than the coherence bandwidth of the channel.

OFDMA uses a large number of narrowband subcarriers compared to a classical multicarrier technique as shown in Figure 3.5. For example, a 20 MHz WCDMA system

with a carrier spacing of 5 MHz bandwidth would support only 4 subcarriers. Further, there is a very tight frequency domain packing of subcarriers with a subcarrier spacing [17]

$$\Delta f = \frac{1}{T_u} \tag{3.1}$$

where T_u is per-subcarrier modulation time. The neighbouring subcarriers overlap with each other in the frequency domain as shown in Figure 3.6, however, it is designed to maintain ideally orthogonality between the subcarriers so that there is no interference between them [23]. The orthogonality also avoids the need of separating subcarriers by guard bands which makes OFDMA spectrally highly efficient.

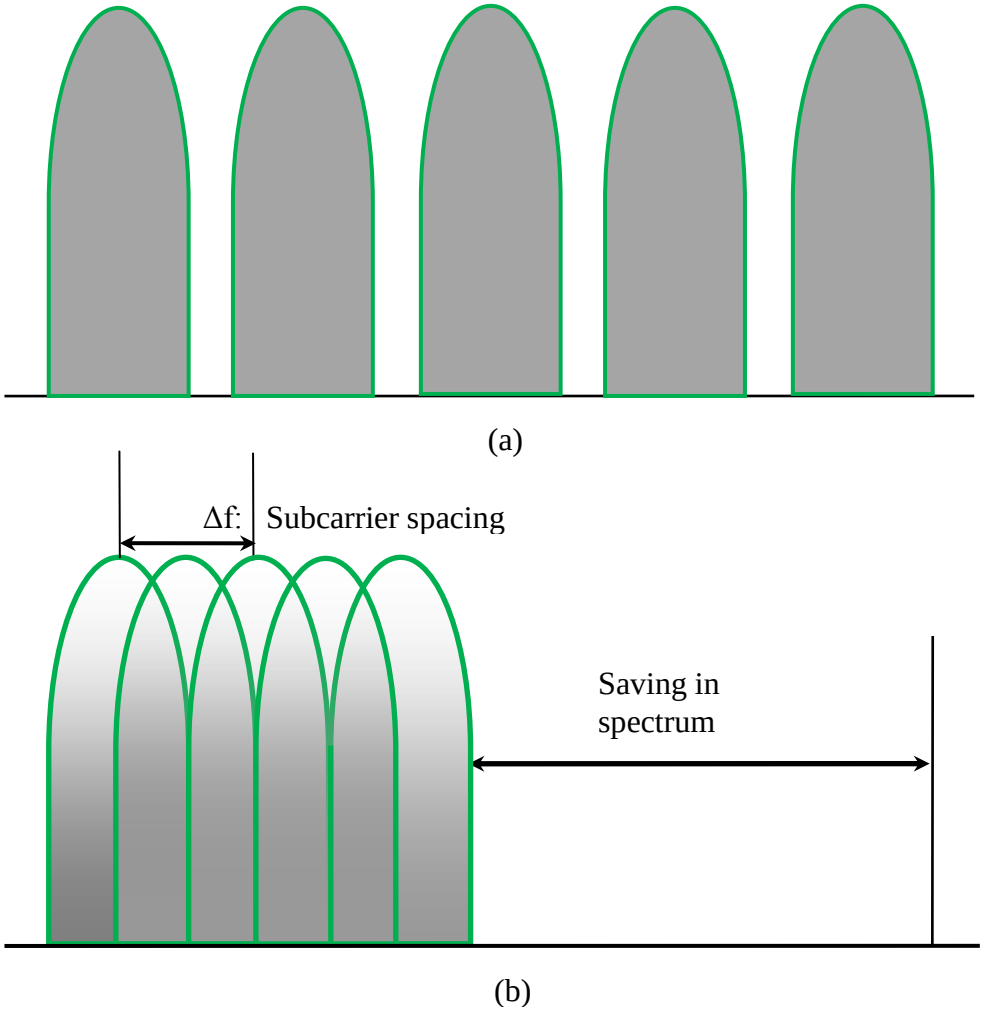

Figure 3.5. *Spectral efficiency of OFDMA compared to classical multicarrier modulation: (a) Classical multicarrier system spectrum (b) OFDMA system spectrum.*

The main reasons for selecting OFDMA as the basic transmission scheme are:

- good performance in frequency selective channels

- high spectral efficiency
- low complexity in the implementation of a baseband receiver
- the ability to easily support advanced features such as link adaptation, frequency domain scheduling and MIMO transmission
- interference mitigation is easier

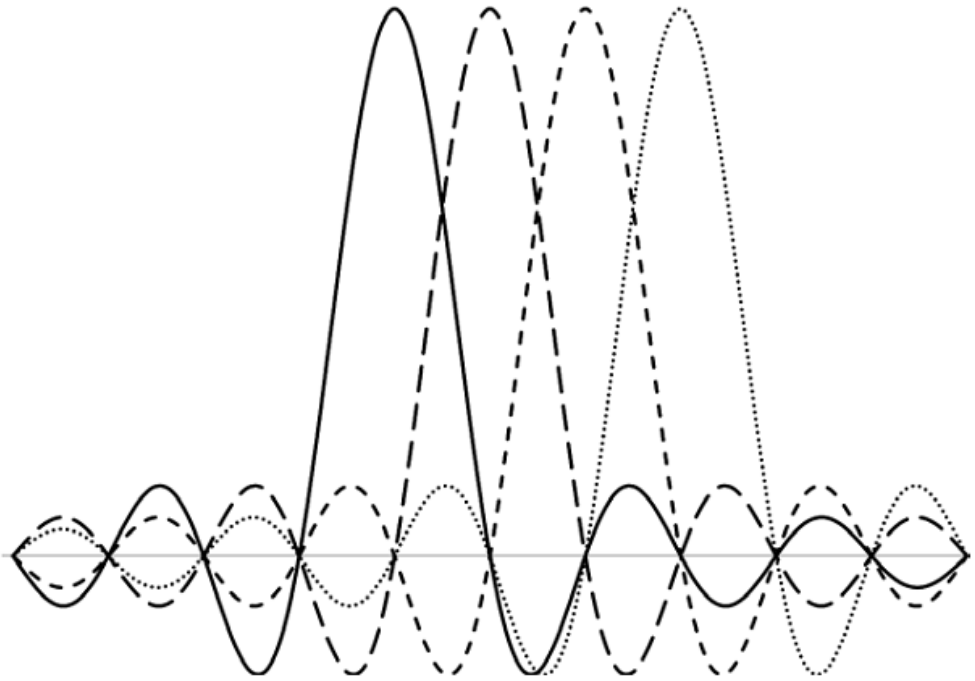

Figure 3.6. *Spectrum of an OFDM symbol consisting of four subcarriers [23].*

In recent years, the OFDMA principle has been widely adopted in varieties of systems such as Digital Video Broadband (DVB), Digital Audio Broadband (DAB), WLANs, Worldwide Interoperability for Microwave Access (WiMAX), and wire line systems like Asymmetric Digital Subscriber Line (ADSL), Very High Bit Rate Digital Subscriber Line (VDSL) and Power Line Communication (PLC).

The practical implementation of OFDM system is based on digital technology and more specifically on the use of the Discrete Fourier Transform (DFT) and the Inverse Discrete Fourier Transform (IDFT) operations. A DFT converts a time domain signal to frequency domain while IDFT performs the reverse task. The size of the Fast Fourier Transform (FFT) is a power of two such as 512, 1024 or 2048. For example, the size of FFT is 2048 for LTE system of 20 MHz bandwidth. In OFDM, the whole available spectrum bandwidth is divided into closely spaced subcarriers. The subcarriers are created by IFFT of the signal at the transmission side as shown in Figure 3.7. A constant frequency difference of 15 kHz is maintained between the subcarriers in LTE Release 8,which gives a symbol duration of

$$1/_{15\ \text{kHz}} = 66.67\ \mu\text{s}.$$

At the transmitter side, data stream is fed to a serial-to-parallel (S/P) converter and then through Subcarrier Mapping (SCM) to an Inverse Fast Fourier Transform (IFFT)

block. The parallel data stream is mapped to a subset of consecutive subcarriers by SCM. The output of the S/P converter is in frequency domain form. IFFT converts them into time domain form and then Cyclic Prefix (CP) is added. Cyclic extension is added by copying a part of the signal end and attaching it to the beginning of the symbol as shown in Figure 3.8. The resulting transformed symbols in parallel then pass through a parallel-to-serial (P/S) converter, digital-to-analog (D/A) converter and finally to the Radio Frequency Transmitter (RF TX).

The reason behind using a CP is to avoid Inter-Symbol Interference (ISI) from the previously transmitted OFDMA symbols. When the length of the CP is greater than the channel impulse response, the effect of the previous symbol can be avoided by removing CP at the receiver side [16]. Note that CP does not carry any data. For a 15 kHz carrier spacing, two types of cyclic prefixes are used: the normal cyclic prefix (4.7 μs) and the extended cyclic prefix (16.7 μs) [24].

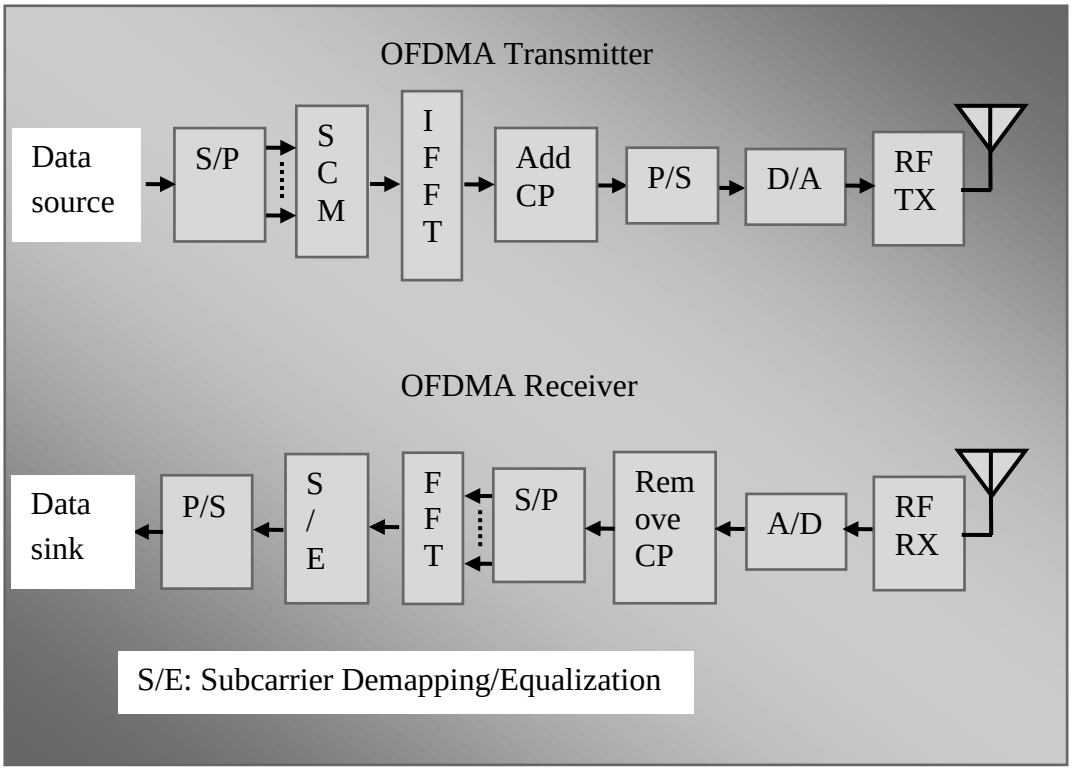

Figure 3.7. *Simplified block diagram of OFDMA transmitter and receiver [23].*

At the receiver side, the receiver performs reverse operation of the transmitter. It uses FFT to recover the original time domain signal. However, before that timing synchronization and frequency synchronization are also performed. Synchronization helps to correct timing frame and OFDM symbol timing. Time synchronization is generally obtained by correlation with known data samples. Frequency synchronization estimates frequency offsets between the transmitter and the receiver.

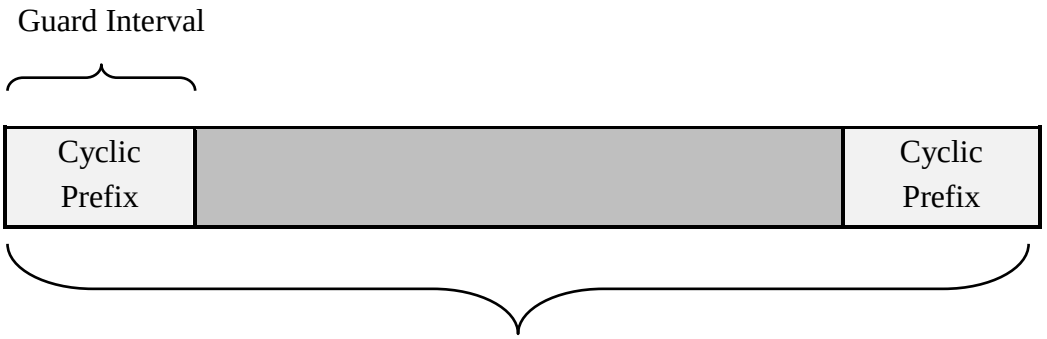

Figure 3.8. *Creation of guard interval for OFDM symbol.*

Although OFDMA offers numerous advantages over other transmission schemes, few challenges are also associated with it. These are:

- **Peak-to-Average Power Ratio (PAPR):** PAPR is defined as the ratio of peak power to average power of the transmitted signal. A high PAPR requires high linearity in the transmitter but linear amplifiers have very low conversion efficiency and therefore are not ideal for mobile uplinks. To solve this problem, SC-FDMA is used in UL, which gives better Power Amplifier (PA) efficiency.
- **Frequency or timing offsets:** Frequency offset in LTE release 8 is tackled by choosing subcarrier spacing of 15 kHz, which gives large tolerance to Doppler shift.

3.2.2 SC-FDMA

One of the major drawbacks of OFDMA is the high value of PAPR. The amplitude variations of the OFDMA modulated signal can be very high. However, practical power amplifiers of the RF transmitters are linear only within a limited dynamic range [20]. Because of this, the OFDMA signal is likely to suffer from non-linear distortion caused by clipping which leads to out-of-band spurious emissions and in-band corruption of the signal. This requires PAs to transmit with high power to avoid such distortion but this would be costly because of expensive RF transmitters. Thus, OFDMA is not used in UL, but instead SC-FDMA is used. SC-FDMA provides similar advantages like OFMDA such as orthogonality among users, frequency domain scheduling and robustness against multipath signal propagation. SC-FDMA requires lower power for amplifier and the PAs have higher conversion power efficiency. This increases coverage in the UL and provides higher UL data rates to the users at the cell edge. This also extends the battery life.

SC-FDMA is a type of single carrier modulation. It is evident from Figure 3.9 that SC-FDMA transceiver has a similar structure to that of OFDMA except the addition of a new DFT block before subcarrier mapping in the transmitter side and IDFT block after subcarrier demapping/equalizer in the receiver side. Hence, SC-FDMA system can be

considered as an OFDMA system with an additional DFT mapper. SC-FDMA modulator transmits symbols sequentially. It divides the sequence of symbols into blocks [25]. As in OFDMA, SC-FDMA also adds CP periodically. But, little difference exits between them. In SC-FDMA CP is not added after every symbol but only at the end of the block.

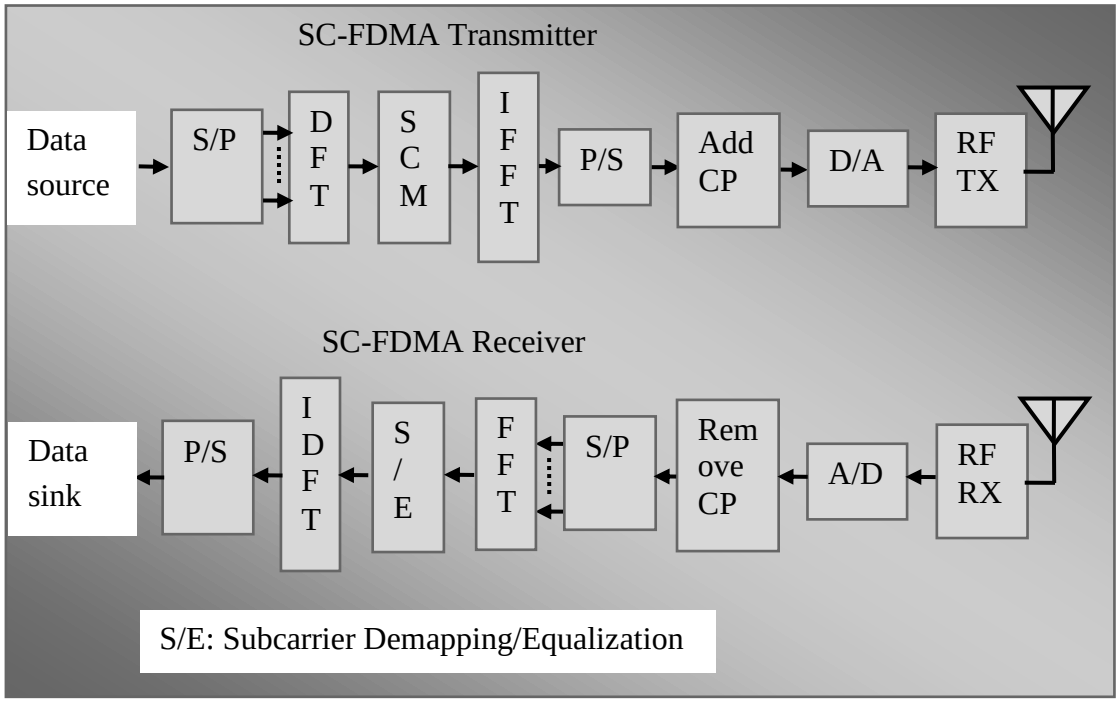

Figure 3.9. *Simplified block diagram of SC-FDMA transmitter and receiver.*

The modulator maps the data bits into modulation symbols and modulated symbols are grouped into data block of N symbols. These blocks of N symbols in time domain are fed to N-point DFT, which transforms them into frequency domain. Frequency domain samples are then mapped into a subset of 12 subcarriers. 12 consecutive subcarriers in one time slot correspond to one UL resource block.

At the receiver side, FFT transforms the received signal into frequency domain. It performs equalization such as Minimum Mean-Square Error (MMSE), decision feedback equalization and turbo equalization in frequency domain. After equalization, IDFT transforms the single carrier signal back to the time domain. At the end, the detector recovers the original modulation symbols. However, OFDMA has a separate detector for each subcarrier [25].

3.3 LTE Frame Structure

As shown in Figure 3.10, LTE frame format is 10 ms in duration and consists of 20 time slots, thus each time slot being 0.5 ms. Two consecutive time slots form one subframe of 1 ms, which is also one Transmit Time Interval (TTI). Each time slot consists of

either seven OFDMA symbols with short/normal CP or six OFDMA symbols with long/extended CP.

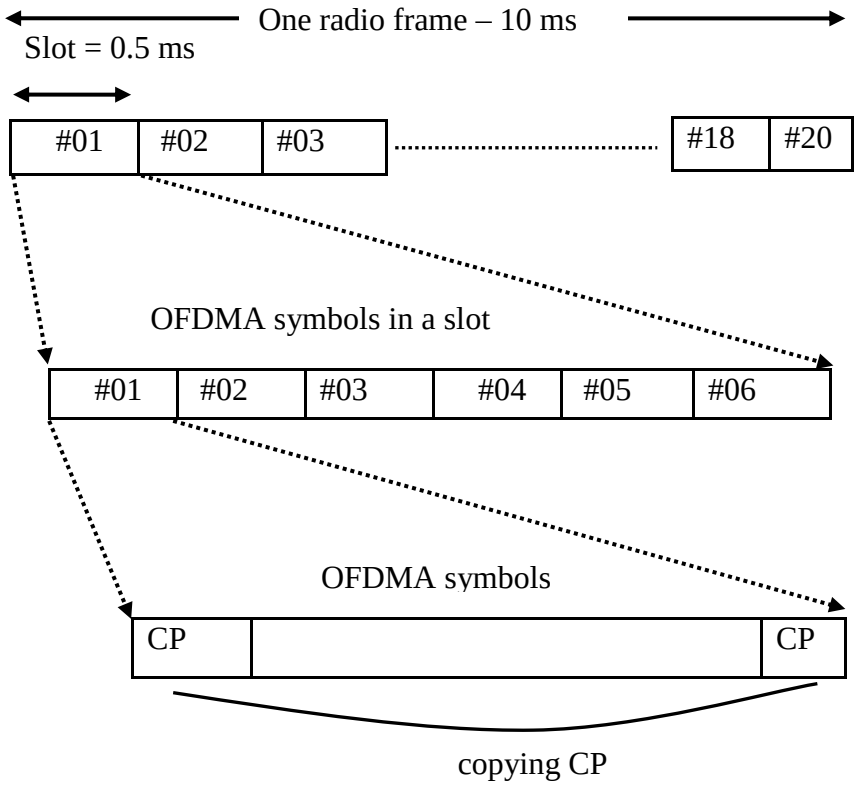

Figure 3.10. *LTE frame structure.*

3.4 User Equipment Measurement Parameters

Different parameters such as Reference Signal Received Power (RSRP), Reference Signal Received Quality (RSRQ) and Signal-to-Noise Ratio (SNR) are used for LTE user performance.

3.4.1 RSRP

RSRP is the most important measurement parameter of UTRAN. RSRP indicates strength of the reference signal power. It is defined as the linear average over power distributions (in watts) of the resource elements that carry cell-specific reference signals within certain frequency bandwidth [20]. RSRP is an important parameter in cell selection/reselection and handover decision making process.

3.4.2 RSRQ

RSRQ indicates the quality of the received reference signal for which RSRP is measured. It plays an important role when RSRP value alone is not sufficient in making cell reselection and handover decisions. RSRQ is defined as [26]:

$$\mathrm{RSRQ} = N \frac{\mathrm{RSRP}}{\mathrm{RSSI}}, \tag{3.2}$$

where N is the number of resource blocks, RSSI is the received strength signal indicator and RSRP is the received signal received power of the signal. RSSI is the total received power including interference from all sources, including serving and non-serving cells, adjacent channel interference and thermal noise [20]. Unlike RSRP, it is measured on all reference elements in the OFDM symbols containing reference signals.

3.4.3 SNR

Signal-to-Interference-plus-Noise ratio (SINR) is one of the important factors for download throughput and is defined as

$$\mathrm{SINR} = \frac{S}{I + N}, \tag{3.3}$$

where S is the average received signal power, N is the noise power and I is the interference power. I is further broken down into

$$I = I_{\mathrm{own}} + I_{\mathrm{other}}, \tag{3.4}$$

where I_{own} is the own cell interference and I_{other} is the other cell interference.
If the power of the interference is zero then SINR reduces to SNR.

4 MEASUREMENT PLAN

The objective of this measurement plan is to demonstrate the effects of user location and movement on signal reception indoors. Correspondingly, the change of user location also has an impact on the load caused to the system network. This chapter describes the environment where measurements were carried out, the test cases, the system tools and the equipment used for the measurement and the procedure used to carry the measurement. Based on this measurement set up, the measured values are analyzed and the measurements results are presented in Chapter 5.

4.1 Measurement Tools and System

The measurements were carried at the indoor location of TUT in the second, third and fourth floor of the Tietotalo building. This was performed because people spend approximately 87 % of their time indoors [27] and the majority of data traffic and calls are carried out indoors [28]. The signal can be received either from an outdoor transmitter or from a transmitter located indoor. This thesis addresses the indoor measurement from the indoor transmitter and could be termed as an indoor to indoor reception.

The LTE system used in the measurements consists of a flexi base station (eNodeB) located at room TC323 in the third floor of the Tietotalo building between the G and H corridors. The eNodeB used for the measurements is manufactured by Nokia Networks and is connected to the core network by means of Gigabit Ethernet cable as shown in Figure 4.1. There were a total of six cells: four outdoor cells (3 micro, 1 macro) and two indoor cells connected to the system. For indoor measurements, only one cell was used and the other cells were disabled during the measurements. One indoor port was connected to the antenna by means of a coaxial cable of 10 m length and 0.5 inches diameter, and an N-type connector. One port of X-pol antenna was used and its other port was terminated. The antenna was supported on a 1.6 m pole on the third floor outside room TC323 near G corridor and was directed along C corridor.

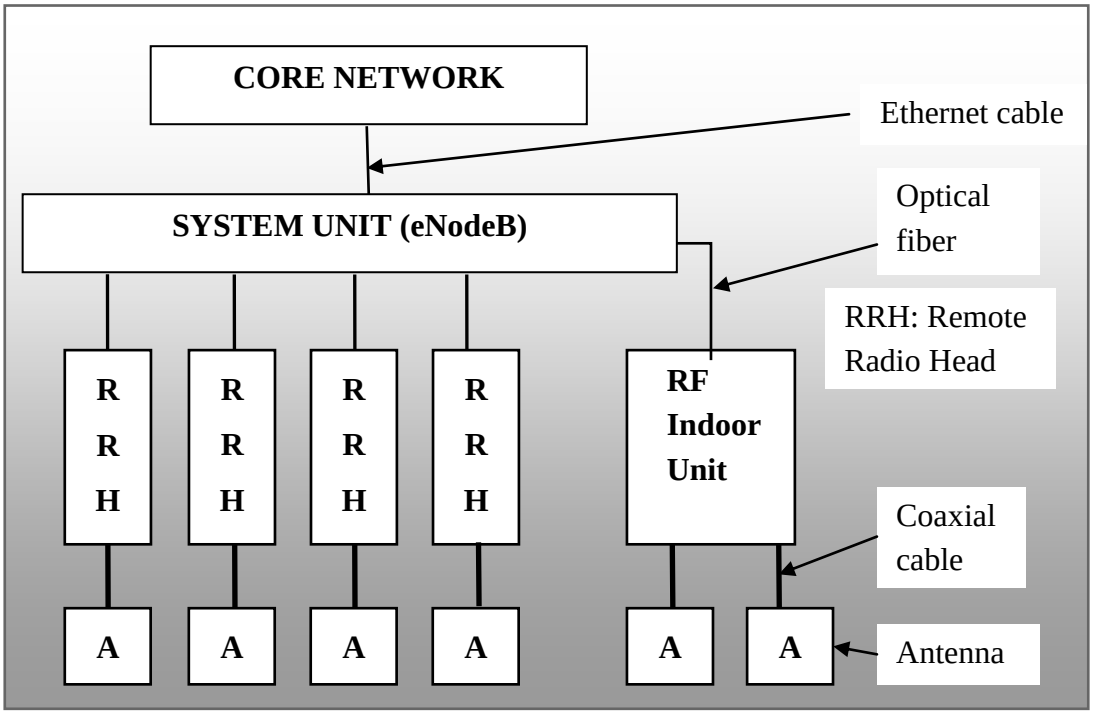

Figure 4.1. *Set up configuration for system.*

Table 4.1. *Parameters of eNodeB set up for measurement.*

Parameter	Value
Carrier Frequency	2100 MHz
UL Carrier	1940
DL Carrier	2130
System Bandwidth	10 MHz
Transmission Power	8 W
LTE Duplex Mode	FDD
No. of Antennas	eNodeB:1, UE:1
Antenna Polarization	+45° or −45° polarization
BTS Antenna Height	1.6 m
MS Antenna Height	1 m

The software inside eNodeB supports LTE Release 8 features. The eNodeB can support bandwidth from 5 MHz to 20 MHz. However, 10 MHz bandwidth was used in these measurements. The system uses Frequency Division Duplex (FDD) multiplexing scheme which means uplink and downlink are separated by frequency bands. The uplink and downlink transmission bandwidths are 1940 MHz and 2130 MHz, respectively. The transmission power of the eNodeB was set to 8 W. Table 4.1 presents the configuration of the eNodeB used for the measurements.

4.2 Measurement Equipment

The measurement equipment consisted of a laptop on a table with an LTE dongle (an LTE data card) attached to it, Nemo Outdoor to collect and Nemo Analyzer to analyze the measurement results. Table 4.2 presents the description of these measurement equipment.

Table 4.2. *Hardware devices and Software used for measurement.*

Measurement Devices	Type	Provider
Laptop	T 161, windows 7	IBM Lenovo
Data Card	LTE Category 3 GSM/GPRS/EDGE/UMTS/LTE Chipset: Qualcomm MDM9200TM Supported frequency bands: 900 MHz, 1800 MHz, 2100 MHz and 2600 MHz Speed: 100/50 Mbps	Huawei E398
Software	Nemo Outdoor 6.3 Nemo Analyzer 6.3	Anite Ltd.

Nemo Outdoor was used for recording the measurements including signaling, data throughput, and all the information flow between eNodeB and UE. These recorded values were saved and used later for further processing. Nemo Analyzer was used for analyzing the measured values and for exporting the data to excel file. The Nemo Analyzer helps to view the data in different forms such as graphs and tables. For further analysis of the data, Microsoft Excel 2007 and MATLAB 7.12.0 (R2011a) were used.

Figure 4.2. *Huawei E398 LTE USB modem used as the UE.*

The LTE dongle, as shown in Figure 4.2, was connected via USB 2.0 to an IBM Lenovo T 161 Laptop with Windows 7 operating system and was used as the receiver (UE). The UE was a Huawei E398 LTE USB modem that is based on Qualcomm MDM9200TM chipset. It is able to operate in 900 MHz, 1800 MHz, 2100 MHz and 2600 MHz frequency bands with different network systems such as GSM, GPRS, EDGE, UMTS and LTE. It can provide a data rate up to 100 Mbps in DL and 50 Mbps in UL direction for LTE 20 MHz frequency band [29]. The TUT LTE eNodeB operates

at LTE band 1, that is, 2100 MHz. The data card is based on LTE UE Category 3 specifications [30]. The modem can support 2x2 MIMO operation and modulation schemes such as QPSK (Quadrature Phase Shift Keying), 16-QAM (Quadrature Amplitude Modulation) and 64-QAM [29]. The UE and eNodeB operate at 2100 MHz and in FDD mode.

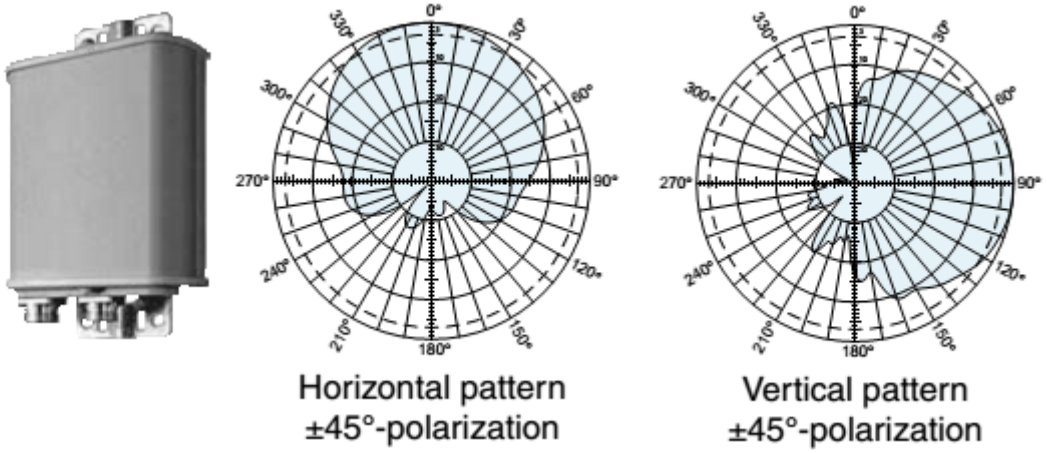

Figure 4.3. *X-pol antenna and its H-Plane and V-Plane HPBWs [31].*

Table 4.3. *X-pol Antenna Specifications [31].*

Parameter	Value
Frequency Range	1710 MHz – 2170 MHz
Impedance	50 ohms
Polarization	+45° and −45°
Gain	8.5 dB – 8.7 dB
VSWR	< 1.4
HPBW	65° (horizontal), 63° (vertical)
Isolation	> 30 dB

The X-pol antenna is a multiband directional X-pol (cross polarization) antenna and was used as a transmitting antenna. It consists of two 45 degree polarized antennas operating at multiband ranging from 1710 MHz to 2170 MHz. The isolation between the ports is greater than 30 dB, which ensures that the mutual coupling effect between the ports is not critical. Voltage Wave Standing Ratio (VSWR) is below 1.4. The Half-Power Beam-Widths (HPBWs) of the horizontal and the vertical pattern of this antenna in the frequency range from 1920 MHz to 2170 MHz are 65° and 63°, respectively. The specification of the antenna is presented in Table 4.3 and its pattern is shown in Figure 4.3.

4.3 Measurement Environment

The measurements were taken along each corridor of the second, third and fourth floor of the Tietotalo building, provided there was proper reception from the transmitting antenna. Figure 4.4 shows the map of the second, third and fourth floor along with static locations. The bullet points in the map indicate points where measurements were taken. There were altogether 13 measurement points: 10 in the corridor, denoted by black bullet points and 3 in the rooms, denoted by red bullet points. The third and fourth floor also has an open space between them. Since the TX antenna is in the third floor, naturally this floor would have better signal level compared to the second and fourth floor. In addition, received signal strength will be stronger at the locations 2, 4, 6 in the third floor as these points are closer to the TX antenna.

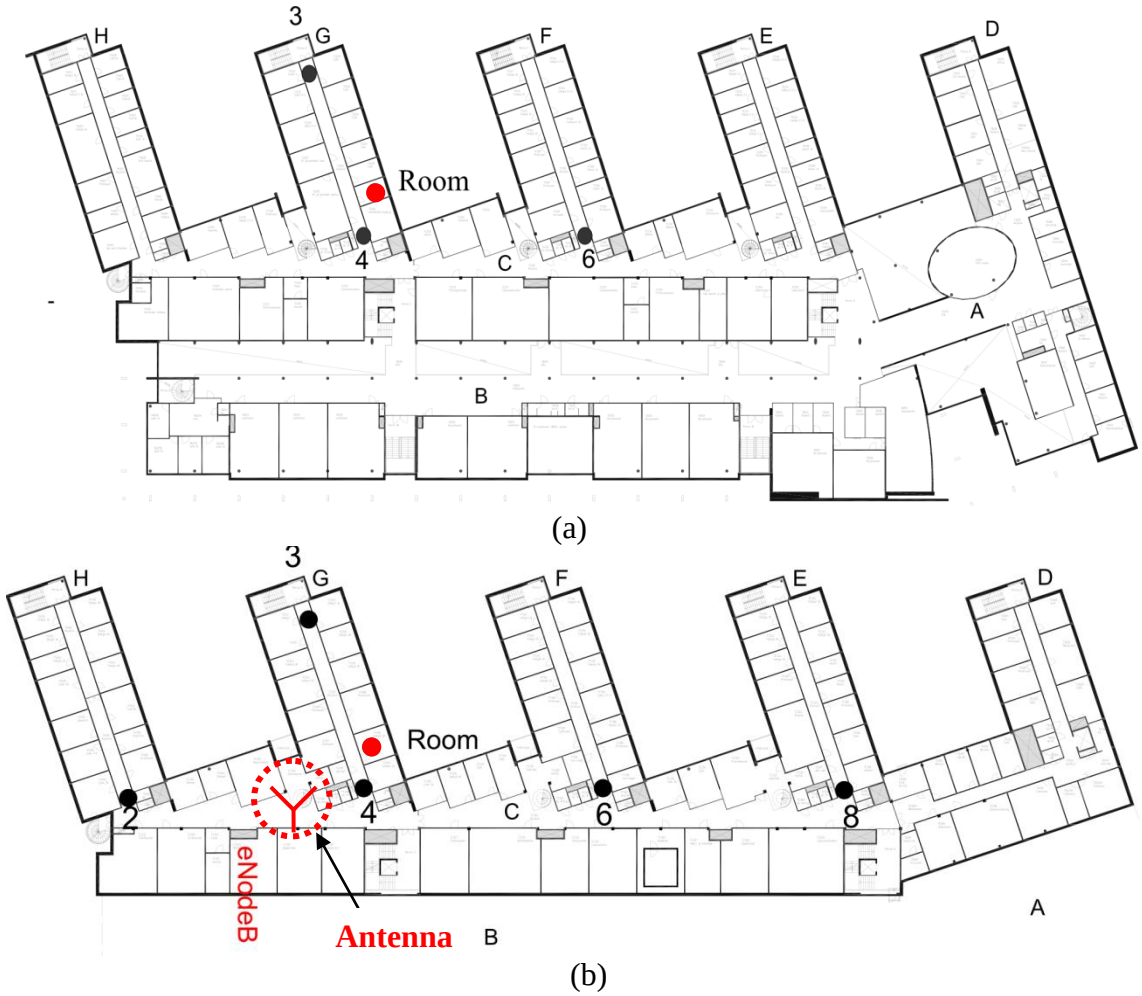

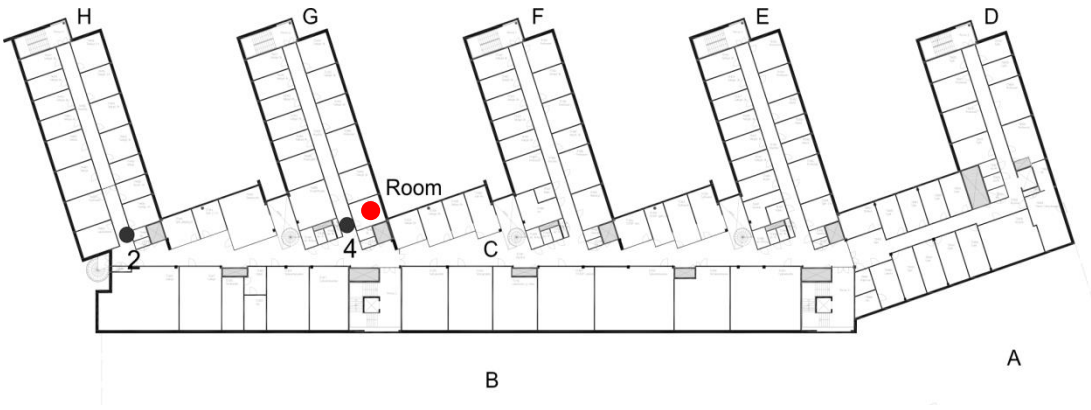

(c)

Figure 4.4. *Tietotalo maps: (a) second floor (b) third floor (d) fourth floor showing measurement points.*

Two static locations (points) were chosen for each corridor as shown in Figure 4.5 – one at the end of the corridor known as the end point and the other one at the entry of the corridor known as the entry point. All the measurement points have different cases.

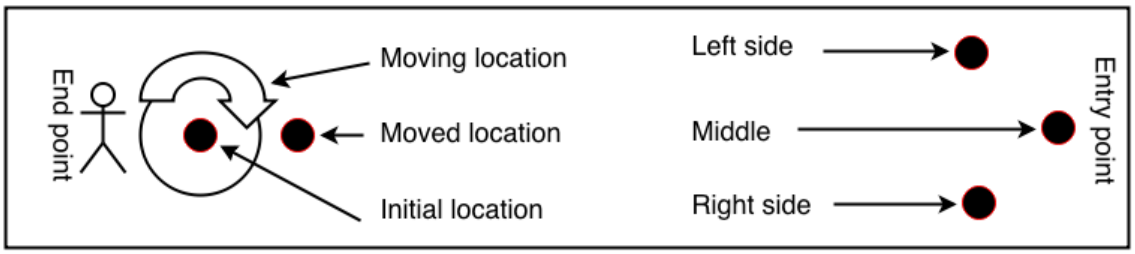

Figure 4.5. Corridor showing static locations and measurement points.

For the end point, three correlating points were selected.

- **Initial location:** This is the initial point of the measurement at the end of the corridor in the middle. In this case, measurement was taken by keeping the measurement equipment stationary.
- **Moving location:** This is the second case of measurement where a person is moving around the measurement equipment at the same position, that is, at the initial location. This was performed to bring more signal variation and to observe how a signal varies when a person is moving around the first location.
- **Moved location:** This is the third case where equipment was moved by a distance of around 1 m away from the first point (Initial location) and it was also kept stationary without any movements.

Entry point also had three correlating points that form a triangular shape as it can be easily seen from Figure 4.5. In this case, the first two measurements were taken at both left and right sides of the corridor and the third one towards C corridor.

- **Left side:** This is the initial point of measurement at the entry of the corridor. In this case measurement was taken by keeping the measurement equipment fixed to the left side of the corridor close to the wall.

- **Right side:** This is similar to the above with user being moved by around 1 m from Initial location to the right side of the corridor close to the wall.
- **Corridor:** In this case, the measurement equipment was moved by a distance of around 1m from the right side towards C corridor into a wider and open space. Thus, the UE was in the vicinity of LoS of the transmitting antenna.

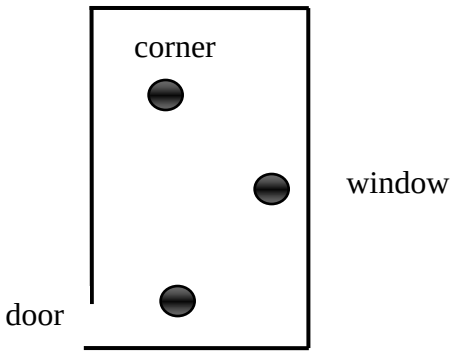

Figure 4.6. *Measurement points inside room.*

Besides measurements in the corridors, few measurements were also taken inside rooms in order to study the effects of user locations at different points in a room. For this, one room in each floor was chosen and measurement equipment was placed on the office table instead of the measurement table. While choosing rooms, it was kept in mind that the rooms should be almost identical in shape and size and had almost similar conditions inside the room as well. These rooms were office rooms that means tables, chairs, books, laptops and around two to three persons were common in each room. During measurements the doors of the rooms were kept partially open but windows (glass windows) in the rooms were closed. All the rooms were chosen in G corridor as there was proper reception for this corridor. Three points were chosen for the measurement inside rooms as shown in Figure 4.6.

- **Near door:** The measurement equipment was placed near door.
- **Near window:** The UE was kept close to a window.
- **At corner:** At this point, measurement was taken by placing the UE at a corner, which was close to the wall near corridor side.

The rooms selected were TG206, TG304 and TG404 in the second, third and fourth floor, respectively.

4.4 Measurement Methods and Set up

A measurement laptop with LTE dongle attached to it and Nemo Outdoor and Nemo Analyzer software running was made ready as shown in Figure 4.7. Figure 4.8 is a schematic representation of the measurement set up configuration. During each measurement, the doors in the corresponding corridor were usually kept closed. Each measurement was recorded by means of Nemo Outdoor for about seven minutes, which gives around 600 to 1100 measurement samples. While plotting these values, 5

percentile and 95 percentile rule was applied which means 5 percent of the values above the minimum value and 5 percent of the values below maximum value were discarded and the rest were used. This was done to avoid unexpected behavior that might have occurred during the measurements and to ensure that any unexpected behavior was not distorting the results. Since the measurements were taken between 9 a.m. and 4 p.m., the people moving here were having an impact to the radio environment.

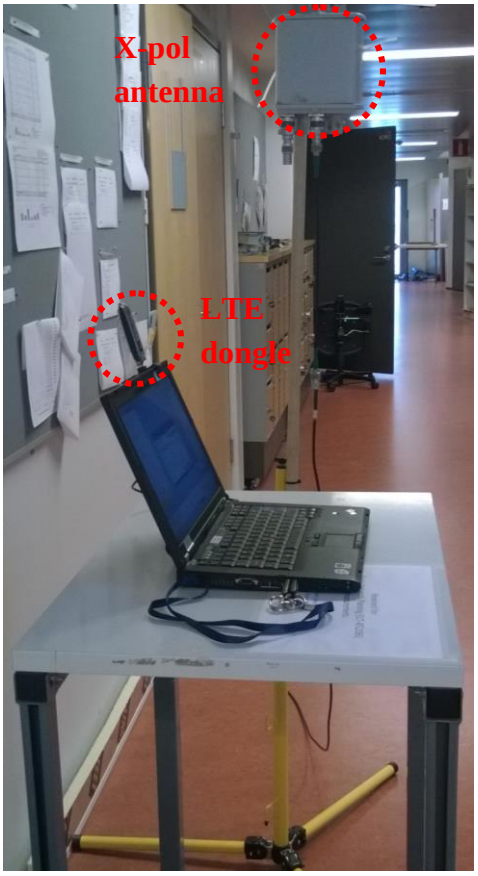

Figure 4.7. *Devices set up for the measurement campaign.*

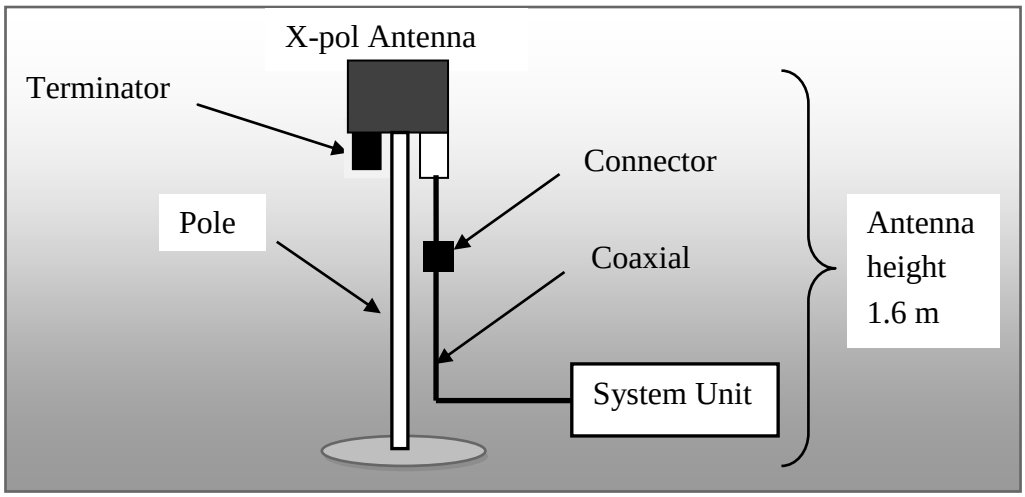

Figure 4.8. *Set up configuration.*

Every measurement was repeated twice so that more measurement data were generated to have more accurate results. The same measurement procedure was followed for each corridor and each room keeping the same device configurations, locations and routes. This was implemented to find similar channel conditions for each measurement.

Some outdoor macro cells were also present during the measurement but it was not possible to lock to a specific cell due to which there was possibility of handovers. However, utmost care was taken to avoid any handover during the measurements.

4.5 Performance Parameters

The main parameters to study were RSRP and SNR. The degree of SNR and RSRP classifies the channel conditions. LTE uses adaptive modulation scheme, which is largely affected by the SNR. Further, the SNR values also affect the throughput. If there is improvement in the RSRP when users are in better locations, then link budget is used to see those effects from the radio network planning point of view.

5 MEASUREMENT RESULTS AND ANALYSIS

Based on the measurement set up explained in Chapter 4, the measurement results are presented in this chapter in terms of RSRP and SNR plots. In addition, the statistical values such as minimum (min), maximum (max), mean, median and standard deviation (s.d.) are also presented in tabular form in dBm (for RSRP) and in dB (for SNR).

Different points (locations) in different corridors and rooms were chosen for measurements, however, only selected points that are more interesting are presented in this chapter. Statistical values of all the measurement points are presented in Appendix B. The whole measurement results can be divided into two cases: Case 1 where measurements were taken in corridors and Case 2 where measurements were taken inside rooms. Further, these are subdivided into the third, second and fourth floor results. These two cases are studied in detail and the results are presented and analyzed in the subsequent chapters.

5.1 Results in the corridor

Third Floor

Five measurement points were taken in the third floor. Results of three points are presented here.

Measurement at point 3 which is at the end of G corridor in the third floor is shown in Figure 5.1 and Table 5.1. Figure 5.1 (a) depicts that both RSRP and SNR values are better when the measurement equipment is moved by 1 m down the corridor. This is as expected because the UE is moving closer to the TX antenna. Measurement at the initial location and moving location has almost identical signal levels. However, signal variations are maximum at the moving location that is when people are moving around the measurement equipment. Moved location has about 1.5 dB better average improvement on initial and moved location. The SNR value is above 19 dB during the whole measurement and reaches to the maximum 29.5 dB.

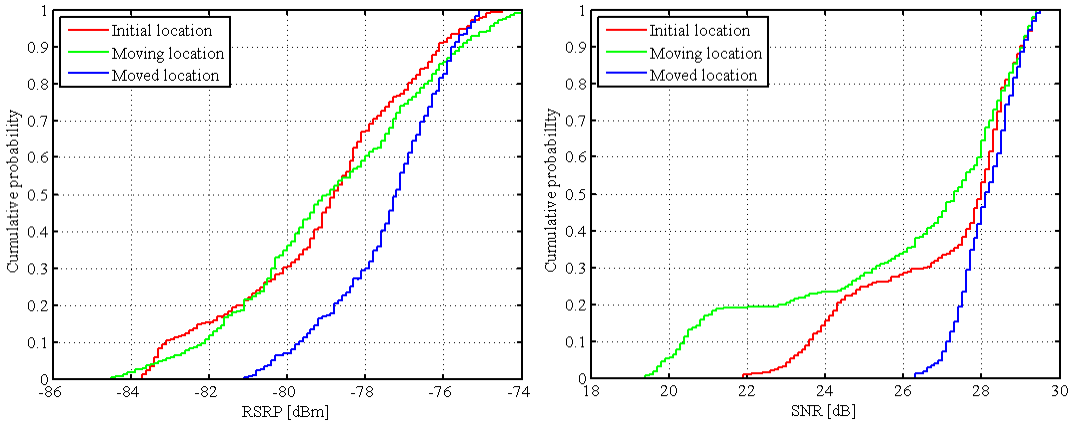

(a) (b)

Figure 5.1. *CDF plot of (a) RSRP (b) SNR at point 3 of G corridor in third floor.*

Table 5.1. *Calculated values of RSRP and SNR at point 3 of G corridor in third floor.*

	Value / Location	Min	Max	Mean	Median	s.d.	Max − Min
RSRP	**Initial location**	−83.70	−74.40	−79.05	−78.80	2.36	9.30
	Moving location	−84.50	−74.00	−78.85	−78.95	2.49	10.50
	Moved location	−81.10	−75.10	−77.43	−77.20	1.46	6.00
SNR	**Initial location**	21.90	29.40	27.03	28.00	2.07	7.50
	Moving location	19.40	29.40	26.05	27.30	3.15	10.00
	Moved location	26.30	29.50	28.12	28.10	0.73	3.20

Next, the measurement was taken at point 4 which is the other end of the same corridor. Figure 5.2 shows a clear benefit in the signal strength as the user location moves towards the more open space than the previous point, where measurement is taken at narrower space. RSRP value ranges from the least value of −66.20 dBm to the peak value of −47.86 dBm, which means 18.34 dB improvement on RSRP could be achieved by staying at the middle than staying at the left side. Table 5.2 shows that the variation of signal levels and the difference between the maximum and minimum value of both RSRP and SNR are the least at the middle location. Compared to the left location, signal level values are stronger when the equipment moves towards the right side of the corridor and gives 8.29 dB average improvement.

The peculiar shape in the SNR plot is seen for measurement at the left side. This can be explained as follows. The measurement at a point was carried twice and these two different results were combined. However, at the other measurement the values were quite different which may be due to interference from other cells most likely from Hermia cells that caused values to be smaller at the other time.

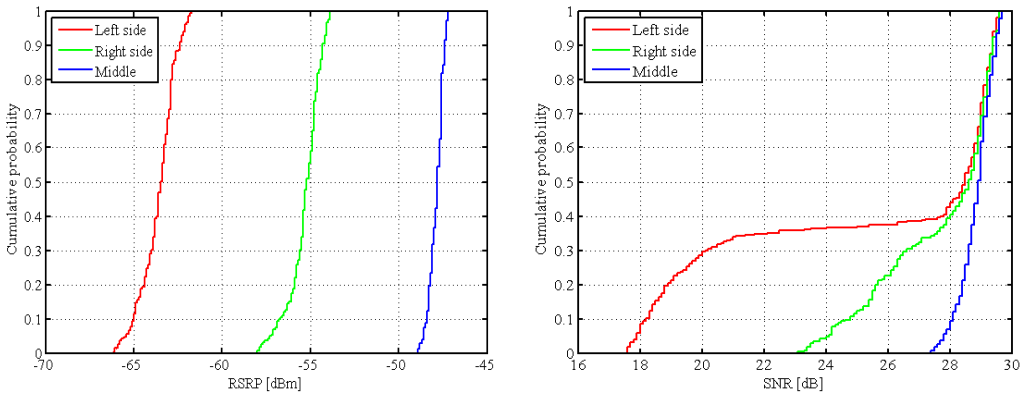

(a) (b)

Figure 5.2. *CDF plot of (a) RSRP (b) SNR at point 4 of G corridor in third floor.*

Table 5.2. *Calculated values of RSRP and SNR at point 4 of G corridor in third floor.*

	Value / Location	Min	Max	Mean	Median	s.d.	Max − Min
RSRP	**Left side**	−66.20	−61.70	−63.60	−63.50	0.98	4.50
	Right side	−58.00	−53.90	−55.31	−55.20	0.91	4.10
	Middle	−48.90	−47.20	−47.86	−47.80	0.39	1.70
SNR	**Left side**	17.60	29.60	25.26	28.50	4.77	12.00
	Right side	23.10	29.60	27.70	28.60	1.84	6.50
	Middle	27.40	29.70	28.85	28.90	0.52	2.30

Figure 5.3 shows the measurement at point 8 at the beginning of E corridor, which is the last measurement in the third floor. Unlike the measurement at point 4, 90 % of the measurement samples for RSRP values at the left side of corridor are greater than that of the right side and are in the range of −88 dBm to −76.5 dBm. However, unlike RSRP values, SNR values for the right location are better. This shows that same pattern was not followed at all the points. The left side provides 2.05 dB improvement in mean RSRP and 3 dB in median RSRP value. During the whole measurement, middle location is dominant just like in point 4. 16.1 dB maximum difference is noted between the worst and the best possible value of RSRP.

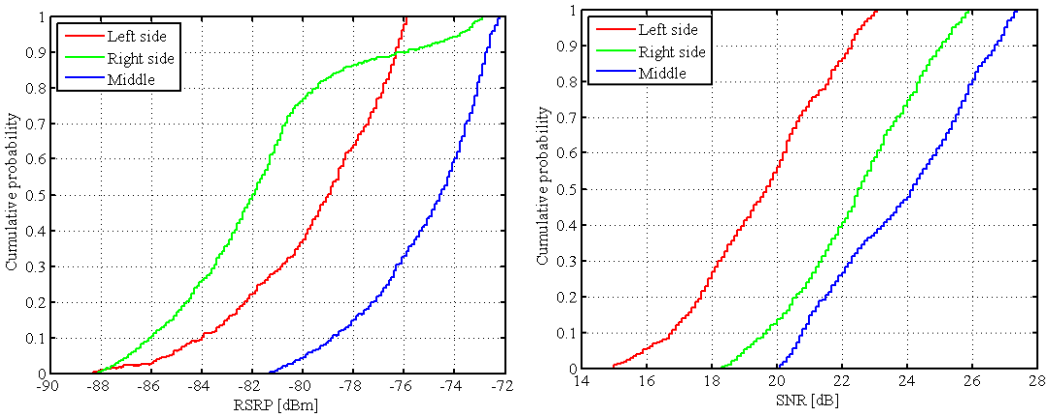

(a) (b)

Figure 5.3. *CDF plot of (a) RSRP (b) SNR at point 8 of E corridor in third floor.*

Table 5.3. *Calculated values of RSRP and SNR at point 8 of E corridor in third floor.*

Value / Location		Min	Max	Mean	Median	s.d.	Max − Min
RSRP	**Left side**	−88.30	−75.90	−79.61	−79.00	2.94	12.40
	Right side	−88.10	−72.90	−81.66	−82.00	3.53	15.20
	Middle	−81.30	−72.20	−75.18	−74.60	2.30	9.10
SNR	**Left side**	15.00	23.10	19.50	19.70	2.03	8.10
	Right side	18.30	25.90	22.47	22.50	1.94	7.60
	Middle	20.10	27.40	23.89	24.20	2.16	7.30

SECOND FLOOR

As it can be seen from Figure 5.4 and Table 5.4, the signal strength has decreased significantly compared to the same location in the third floor. This is quite intuitive because the signal reaches to the second floor by passing through different walls and floors. Difference between the minimum and maximum RSRP signal level is the greatest for moved location. However, similar behavior is not seen in SNR. Moved location has better SNR all the times. Variance of SNR values is least in this case. By moving a little bit down the corridor, a maximum 9 dB difference is noted in SNR. When compared to the same point in the third floor, the maximum value of RSRP is 25.9 dB lower than the maximum value of RSRP in the third floor.

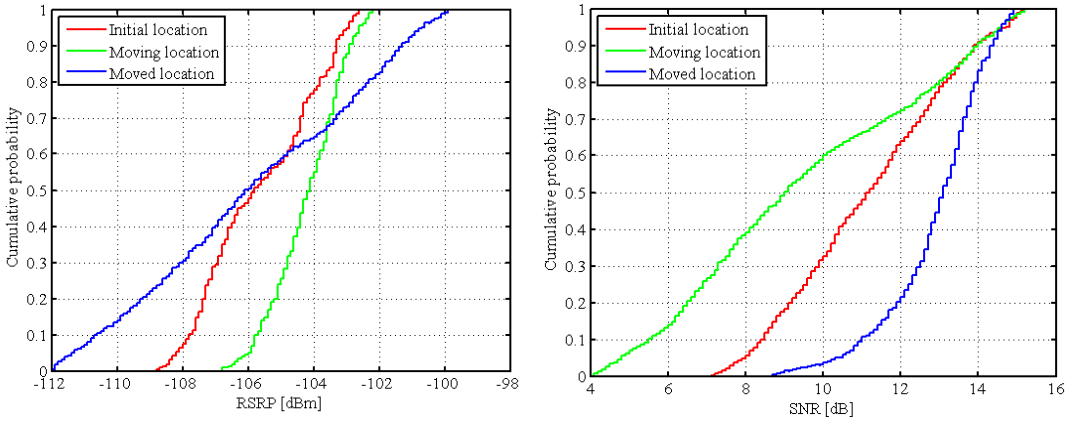

(a) (b)

Figure 5.4. *CDF plot of (a) RSRP (b) SNR at point 3 of G corridor in second floor.*

Table 5.4. *Calculated values of RSRP and SNR at point 3 of G corridor in second floor.*

	Value / Location	Min	Max	Mean	Median	s.d.	Max − Min
RSRP	**Initial location**	−108.80	−102.60	−105.62	−105.80	1.72	6.20
	Moving location	−106.80	−102.20	−104.20	−104.10	1.06	4.60
	Moved location	−112.00	−99.90	−105.84	−106.10	3.39	12.1
SNR	**Initial location**	7.10	15.20	11.18	11.20	2.05	8.10
	Moving location	4.10	15.20	9.49	9.00	3.12	11.10
	Moved location	8.70	14.90	12.88	13.10	1.28	6.20

Figure 5.5 and Table 5.5 show that surprisingly, the middle location is not the best location at the other end of G corridor. Despite the middle location being at more open space, the multipath components have added constructively at the left side of corridor resulting better signal level for most of the time. This also shows that best location does not exist all the time. At middle location, variance in RSRP values is the least but maximum for SNR. By staying at the left location, a large difference of 13.6 dB is noted between the minimum and maximum value of RSRP. On the other hand, the peculiar shape more likely has caused due to handover to other outdoor macro cell during the measurement.

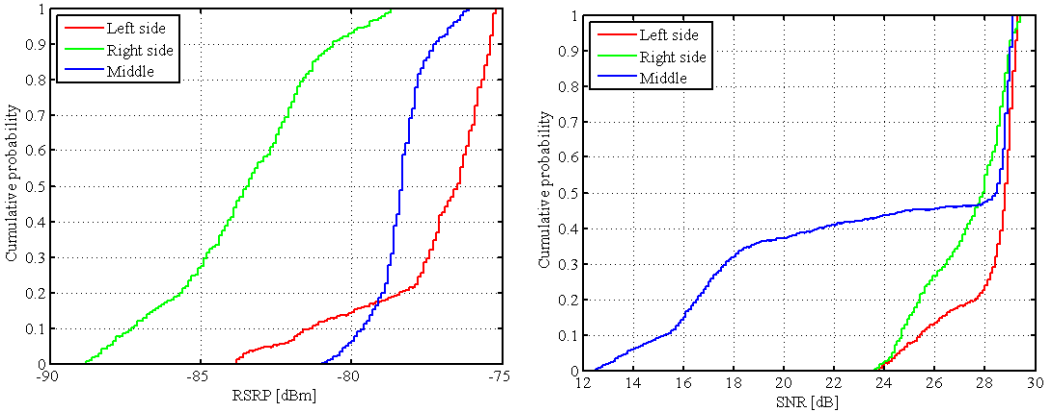

(a) (b)

Figure 5.5. *CDF plot of (a) RSRP (b) SNR at point 4 of G corridor in second floor.*

Table 5.5. *.Calculated values of RSRP and SNR at point 4 of G corridor in second floor.*

	Value / Location	Min	Max	Mean	Median	s.d.	Max − Min
RSRP	**Left side**	−83.80	−75.20	−77.33	−76.50	2.22	8.60
	Right side	−88.80	−78.70	−83.60	−83.40	2.44	10.10
	Middle	−81.00	−76.10	−78.37	−78.30	0.92	4.90
SNR	**Left side**	23.80	29.30	28.16	28.80	1.45	5.50
	Right side	23.60	29.40	27.29	27.90	1.64	5.80
	Middle	12.50	29.10	23.57	28.50	6.05	16.60

At point 6 of the second floor, the signal has almost same value at the left and right side of the corridor as shown in Figure 5.6 and Table 5.6. However, the SNR value at the right side is approximately 2 dB greater at all the points. Variance of RSRP and SNR values is least at the left side. A maximum improvement of 10.7 dB is noted by moving towards the C corridor.

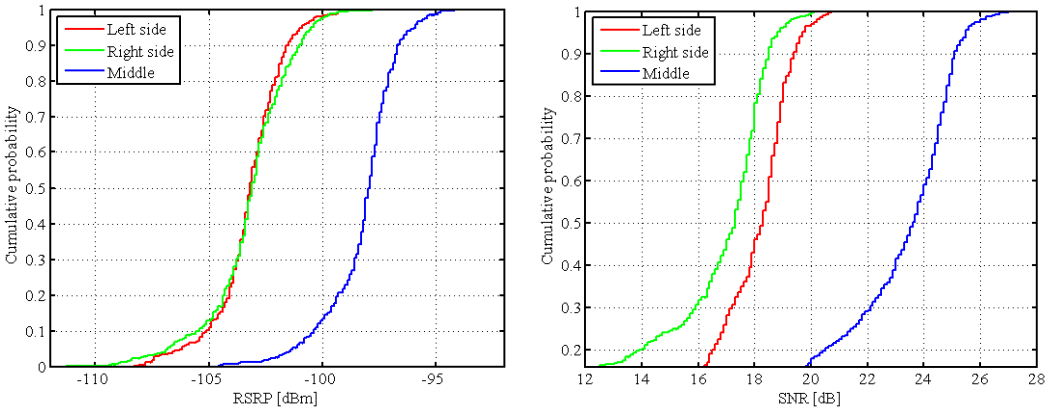

(a) (b)

Figure 5.6. *CDF plot of (a) RSRP (b) SNR at point 6 of G corridor in second floor*

Table 5.6. *Calculated values of RSRP and SNR at point 6 of F corridor in second floor.*

	Value / Location	Min	Max	Mean	Median	s.d.	Max − Min
RSRP	**Left side**	−106.10	−101.00	−103.17	−103.20	1.05	5.10
	Right side	−106.70	−100.50	−103.10	−103.10	1.31	6.20
	Middle	−101.20	−96.00	−98.13	−97.90	1.10	5.20
SNR	**Left side**	15.00	19.60	17.91	18.30	1.14	4.60
	Right side	8.70	18.80	16.15	17.30	2.78	10.1
	Middle	18.80	25.40	22.97	23.60	1.91	6.6

FOURTH FLOOR

The fourth floor has less number of points compared to the third and second floor. This is because the signal strength was poor and making handover to the other cells. However, at some locations, such as G corridor, the signal strength was still good due to the open space between G corridors of the third and fourth floor.

Figure 5.7 and Table 5.7 present measurement point 4 in G corridor. RSRP and SNR values are decreasing in the fourth floor compared to the corresponding G corridor in the third floor. However, it is stonger compared to the second floor at this point. This is because the signal has to pass through less number of walls due to the open space between the third and fourth floor. Here, the average values of RSRP and SNR are about −80 dBm and 25 dB respectively. Middle location provides average gain of around 8 dB compared to the left location and around 6 dB compared to the right location. The standard deviation values are least for right location. The maximum and minimum RSRP values have a 13 dB difference. When compared to the same point in the second floor, there is about 14.4 dB difference in the minimum signal strength values.

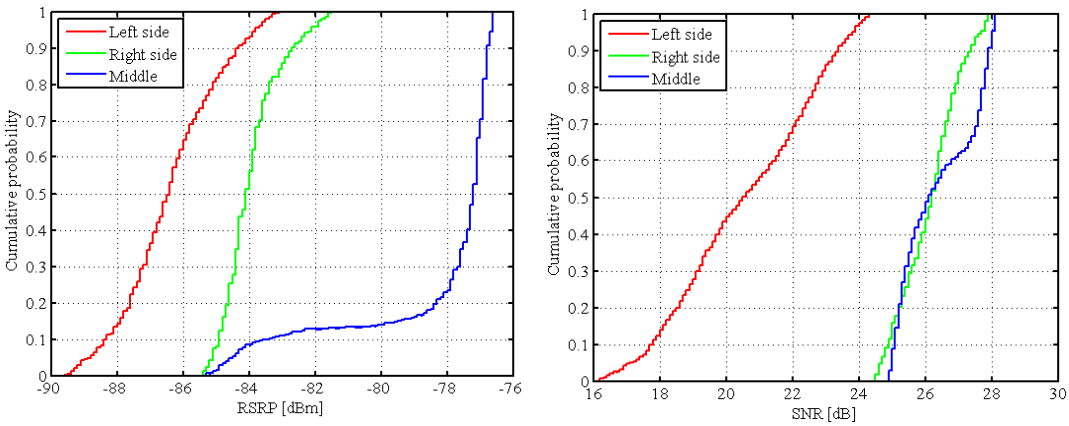

(a) (b)

Figure 5.7. *CDF plot of (a) RSRP (b) SNR at point 4 of G corridor in fourth floor.*

Table 5.7. *Calculated values of RSRP and SNR at point 4 of G corridor in fourth floor.*

	Value / Location	Min	Max	Mean	Median	s.d.	Max − Min
RSRP	**Left side**	−89.60	−83.10	−86.39	−86.40	1.46	6.50
	Right side	−85.40	−81.50	−83.93	−84.10	0.85	3.90
	Middle	−85.30	−76.60	−78.19	−77.20	2.39	8.70
SNR	**Left side**	16.20	24.30	20.57	20.50	2.11	8.10
	Right side	24.50	27.90	26.13	26.20	0.89	3.40
	Middle	24.90	28.10	26.41	26.10	1.14	3.20

Figure 5.8 indicates measurement at the entry of the H corridor. Like other corridors, middle location is providing better signal strength compared to measurement at the left and right side of the corridor. SNR here is following the same pattern as of RSRP. However, standard deviation of both RSRP and SNR is large at the middle location. Right location provides 4.63 dB average improvement over the left location. At this point a large difference of 23.1 dB is noted between the best and worst value of RSRP.

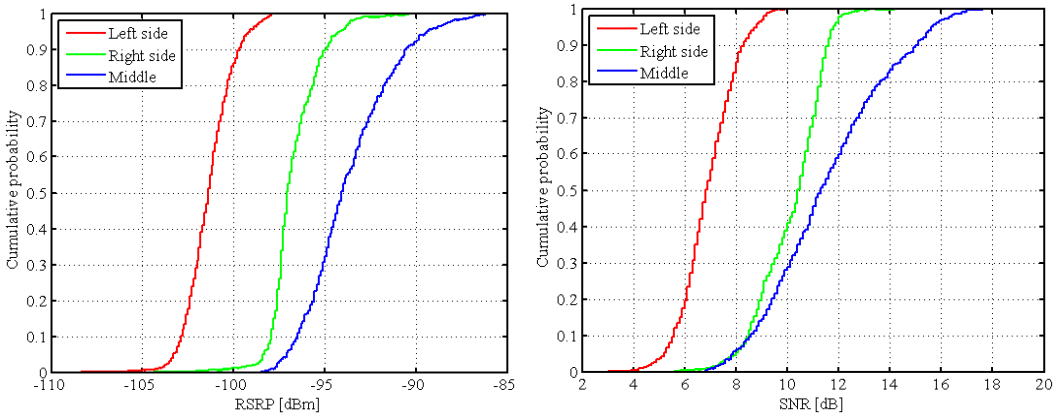

(a) (b)

Figure 5.8. *CDF plot of (a) RSRP (b) SNR at point 2 of H corridor in fourth floor.*

Table 5.8. *Calculated values of RSRP and SNR at point 2 of H corridor in fourth floor.*

	Value / Location	Min	Max	Mean	Median	s.d.	Max − Min
RSRP	**Left side**	−108.40	−97.90	−101.33	−101.40	1.28	10.50
	Right side	−104.4	−90.10	−96.70	−97.10	1.39	14.30
	Middle	−98.50	−85.30	−93.66	−94.10	2.38	13.20
SNR	**Left side**	3.00	10.10	6.91	6.80	1.07	7.10
	Right side	5.60	14.90	10.17	10.40	1.27	9.30
	Middle	6.80	18.30	11.56	11.30	2.35	11.50

5.2 Results inside rooms

Figure 5.9 shows measurement inside a room in the third floor. At this point, signal strength is better near the door, followed by the measurement at the corner and the window. The minimum value of signal level at door location is greater than the maximum of other the two cases. By staying near the door, an average improvement of 7.91 dB to 10.02 dB can be obtained. The average value of RSRP at corner is about 1 dB higher than that near window. This is because corner location is closer to the corridor.

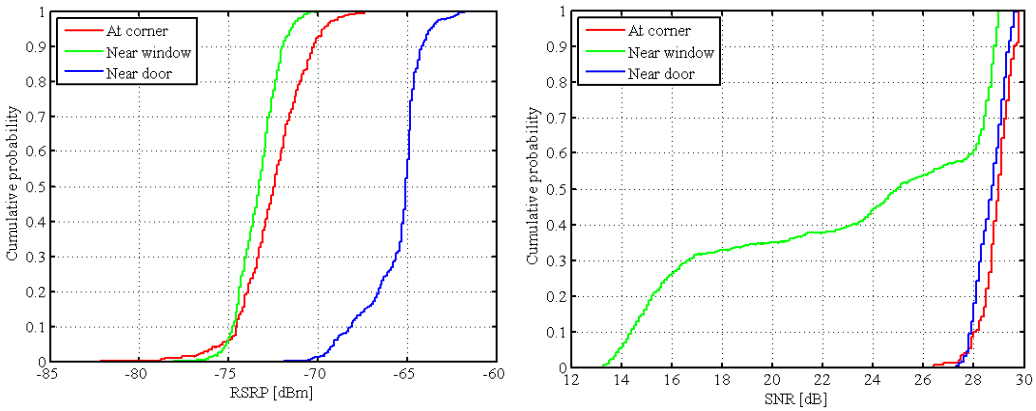

(a) (b)

Figure 5.9. *CDF plot of (a) RSRP (b) SNR inside a room in third floor.*

Variance of SNR values is large near the window. SNR curve near the door and at the corner follow each other and they have average value of approximately 28 dB. SNR values remain above 20 dB during most of the measurement. The strange shape of SNR value near window might have caused due to the movement of people in the room at that time or due to change in the orientation of the TX antenna. Nevertheless, about 50 % of the samples near the window have SNR values below 25 dB.

Table 5.9. *Calculated values of RSRP and SNR inside a room in third floor.*

	Value / Location	Min	Max	Mean	Median	s.d.	Max − Min
RSRP	**At corner**	−75.30	−69.70	−72.44	−72.40	1.34	5.60
	Near window	−75.00	−71.60	−73.33	−73.30	0.88	3.40
	Near door	−68.90	−63.70	−65.42	−65.10	1.13	5.20
SNR	**At corner**	26.40	29.80	28.91	29.00	0.61	3.40
	Near window	13.30	29.00	22.95	25.00	5.96	15.70
	Near door	27.30	29.70	28.66	28.70	0.57	2.40

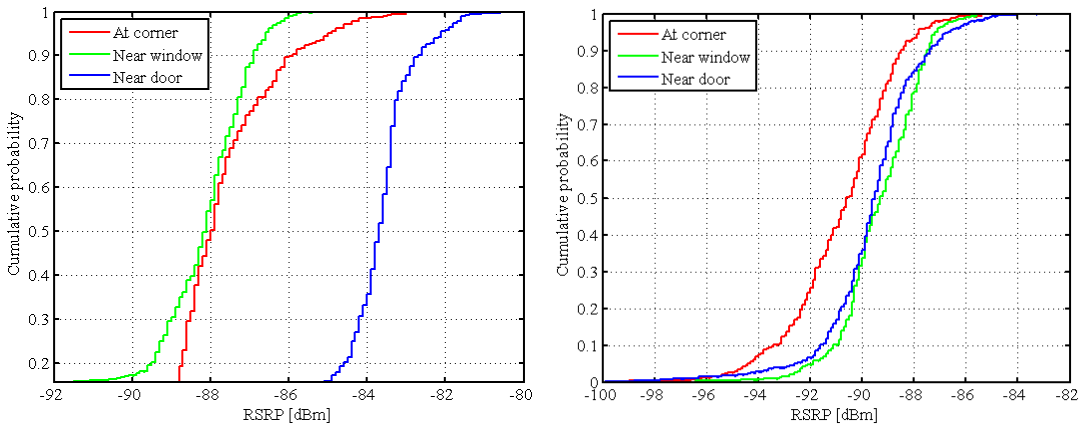

(a) (b)

Figure 5.10. *CDF plot of RSRP inside a room in (a) fourth (b) second floor.*

Similar to the nature of curve in Figure 5.9 (a) is obtained when measured at a room in the fourth floor. As can be seen from Figure 5.10 (a), the strongest signal strength is near door followed by that at the corner and near the window. Table 5.10 shows that the variance of the signal is very less near the door and at the corner. 18.5 dB difference between the maximum value of RSRP in the third and fourth floor and 23.1 dB between the third and second floor is obtained.

Table 5.10. *Calculated values of RSRP and SNR inside a room in fourth floor.*

	Value / Location	Min	Max	Mean	Median	s.d.	Max − Min
RSRP	**At corner**	−89.20	−85.00	−87.78	−87.95	0.97	4.20
	Near window	−115.30	−86.70	−91.39	−88.20	8.74	28.6
	Near door	−86.90	−82.20	−83.90	−83.70	0.89	4.7
SNR	**At corner**	21.70	26.50	24.38	24.70	1.29	4.80
	Near window	3.20	25.80	16.79	15.20	6.55	22.60
	Near door	22.60	27.90	25.86	26.30	1.46	5.30

Table 5.11. *Calculated values of RSRP and SNR inside a room in second floor.*

	Value / Location	Min	Max	Mean	Median	s.d.	Max − Min
RSRP	**At corner**	−94.30	−87.90	−90.71	−90.60	1.53	6.40
	Near window	−91.70	−87.30	−89.23	−89.30	1.12	4.40
	Near door	−92.50	−86.80	−89.52	−89.50	1.21	5.70
SNR	**At corner**	23.10	27.20	25.53	25.60	0.98	4.10
	Near window	17.10	25.50	21.68	21.80	2.68	8.40
	Near door	17.30	26.70	21.68	21.40	3.08	9.40

Figure 5.10 (b) shows the measurement inside the room in the second floor. RSRP values do not have much differences. The maximum value of RSRP is still near door just like the room in the third and fourth floor. However, unlike third and fourth floor, the signal strength of RSRP at the corner is the weakest but its SNR value is greater than the other two cases. 7.5 dB difference occurs between the weakest and the strongest value of RSRP as seen from Table 5.11.

6 CONCLUSIONS AND DISCUSSION

The aim of this thesis was to study signal reception from indoor transmitter to indoor environment and how the variations in the user location and movement of a person around the measurement equipment affect the received signal levels. Firstly, the measurements were carried out at the beginning and end of different corridors in different floors, and later inside rooms, one in each floor in the Tietotalo building of TUT.

A number of observations are noted based on the measurement results. A slight change in the user terminal location had a noticeable impact on the received signal levels. RSRP and SNR values were stronger in more open and wider spaces, and near the transmitting antenna.

Signal levels were higher in the third floor with RSRP value up to about −50 dBm and SNR value up to 30 dB. This was natural because the transmitting antenna was located in the third floor. As the signal passed through different walls and floors, RSRP and SNR values were noted lower in the second and fourth floor; the RSRP value had decreased to −110 dBm and the SNR value to 3 dB.

When measuring in the office rooms, the best received signal power level was observed near the door compared to the RSRP value near the window and near the corner. However, SNR values were generally better near the corner. Signals levels were the weakest and most fragmented near the window most of the times. This is likely due to losses in materials of the windows. Ari Asp et al. in [32] [33] suggest that modern windows in Finland are three to four layered made of high energy efficient materials such as low emission glasses that cause substantial penetration losses in the order of 26–35 dB. The received signal level, between the worst and best value of RSRP, could be improved by 7–11 dB by staying near the door. Further, the measured average value of the RSRP near door was about 4–8 dB higher than the other two locations inside a room.

At the end point of every corridor, both RSRP and SNR values were mostly the highest when the measurement equipment was moved down towards C corridor. The received signal strength at the moved location was on average 2 dB better than that of the initial and the moving location. RSRP and SNR values were usually lower at the moving case, that is, when a person was moving around the equipment. More often, the received signal was also quite fragmented at the moving location. This suggests that it is preferred to choose location where people are not moving around. 10–12 dB and 9–10 dB difference between the strongest and weakest value of RSRP and SNR were obtained, respectively at the end point of the corridors.

On the other hand, at the entry point of each corridor, average improvement at the middle location was better compared to the measurement at the left and the right side of the corridor. This is because the middle location that is at relatively more open space several multipath components are received at that location in comparison with sides of a corridor where there are most likely less multipath components. The average improvement of RSRP value at the middle of the corridor was recorded to be approximately 14 dB in the third floor and decreased to 6 dB in the second floor and to about 8 dB in the fourth floor as explained in Appendix A. Thus, it also shows that the improvement at the beginning of the corridor was higher than at the end of the corridor. A large improvement up to 10–23 dB was noted at the middle location as shown in Appendix C.

Based on the improvement from the optimized location, a number of benefits could be achieved not only from the user point of view but also from the operator's point of view. Users could be guided to optimize their UE location based on signal strength and connection quality. In addition, this optimization reduces energy consumption at the UE and eNodeB, and thus minimizes radiation, reduces battery consumption of mobile terminals, reduces cost and increases capacity.

The location of BSs is generally not known to the users. However, with the help of some mechanisms such as Mobile Performance Gaming (MPG) [34], or by using some applications on their smartphones, users can monitor the signal strength, approximate the BS location, and choose the optimized location directly. This would not only allow users to avoid bad locations but also guide them to better signal connection quality whenever possible. But again, this does not mean to limit the mobility of the users as they prefer to have seamless connectivity and better quality services everywhere.

Measurements were conducted mostly during day time and by keeping UE height fixed. A way to get more results could be implemented by considering the effects of user locations also in the night time and in addition by varying the heights of UE.

Some errors are possible on the results as the measurements were not taken in the ideal environments. These errors are possibly due to handovers to the other cells, most likely from Hermia cells or movement of people close to the TX antenna or change in the measurement set up. Movement of people probably has not caused large distortions in the signal levels as they passed quickly. Nevertheless, 5 percentile and 95 percentile rule was employed to ensure that any unexpected behaviour was not distorting the measurement results.

As a conclusion, from users' perspective it is beneficial for them to choose wider and more open spaces and preferably locations where no people is moving around.

The measurements were carried out in the Tietotalo building, however, it is expected similar behaviors would be obtained in other buildings, provided similar methods are followed.

REFERENCES

[1] S. Kumar Das, *Mobile Handset Design*, John Wiley & Sons (Asia) Pte Ltd, 2010.

[2] Timo Halonen, Javier Romero and Juan Melero, GSM, *GPRS and EDGE Performance*, *Evolution towards 3G/UMTS*, John Wiley & Sons, Ltd second edition, 2003.

[3] 2G and 3G cellular networks: Their impact on today's enterprise mobility solutions and future mobility strategies. White Paper, Motorola.

[4] S. Patil, V. Patil, and P. Bhat, "A Review on 5G Technology" International Journal of Engineering and Innovative Technology, vol 1 Issue 1, January 2012.

[5] Samsung Tomorrow, Samsung Electronics Official Global Blog [WWW]. Accessed on [02.10.2014]. Available at: http://global.samsungtomorrow.com/?p=43349

[6] T. Rappaport, *Wireless Communications Principles and Practice,* Prentice Hall, second edition, 2002.

[7] J. Lempiäinen, M. Manninen, *Radio Interface System Planning for GPSM/GPRS/UMTS,* Kluwer Academic Publishers, 2002.

[8] B. H. Fleury, P.E. Leuthold, "Radio Propagation in Mobile Communications: A Review of European Research", *IEEE Communications Magazine*, February 1996.

[9] S.R. Saunders, A. A. Zavala, *Antennas and Propagation for Wireless Communication Systems,* Wiley, second edition, 2007.

[10] A. F. Molisch, *Wireless Communications*, Willey, second edition, 2011.

[11] A. Goldsmith, *Wireless Communications,* Cambridge University Press, 2005.

[12] M. Hata, Empirical formula for propagation loss in land mobile radio services, *IEEE Transactions on vehicular Technology,* 29, 317-25, 1980.

[13] European Cooperative in the Field of Science and Technical Research EURO-COST 231, "Urban transmission loss models for mobile radio in the 900 and 1800 MHz bands," Revision 2, The Hague, Sept. 1991.

[14] 3GPP, Overview of 3GPP Release 99, Summary of all Release 99 Features.

[15] M. Sauter, *From GSM to LTE – An Introduction to Mobile Networks and Mobile Broadband,* John Wiley & Sons, Ltd, first edition, 2011.

[16] Tara Ali-Yahiya, *Understanding LTE and its performance*, Springer.

[17] H. Holma, A. Toskala, *LTE for UMTS Evolution to LTE- Advanced,* Willey, second edition, 2011.

[18] A. Ghosk, R. Ratasuk, *Essentials of LTE and LTE-A,* Cambridge University Press, 2011.

[19] E. Dahlman, S. Parkvall, J. Sköld, P. Beming, 3G Evolution: *HSPA and LTE for Mobile Broadband*, second edition, 2008.

[20] S. Sesia, I.Toufik, M. Baker, *LTE – the UMTS Long Term Evolution – From Theory to practice,* John Willey & Sons Ltd., second edition, 2011.

[21] 3GPP TS 23.203, Policy and charging control architecture, v10.1.0, September 2010.

[22] Holma, H. and Toskala, A., WCDMA for UMTS – HSPA Evolution and LTE, John Wiley & Sons, Ltd, 4th edition, 2007.

[23] S.C. Yang, *OFDMA System Analysis and Design,* Artech House, 2010.

[24] C. Johnson, *Long Term Evolution in Bullet,* first edition, 2010.

[25] H.G. Myung, D.J. Goodman, *Single Carrier FDMA – New Air Interface For Long Term Evolution,* John Willey and Sons, Ltd, first edition, 2008.

[26] LTE Quick Reference, Share TechNote. [WWW]. Accessed on [15.06.2014]. Available at: http://www.sharetechnote.com/html/Handbook_LTE_RSRQ.html

[27] N. Klepeis et al. The National Human Activity Pattern Survey (NHAPS): a resource for assessing exposure to environmental pollutants *J. Expo. Anal. Environ. Epidemiol.* , 11(3): 231–252, May-Jun 2001.

[28] A. Mason, "The message from MWC 2010: indoor coverage and subscriber management are the keys to dealing with exponential growth in wireless traffic", 2010.

[29] Huawei. Huawei E398 Specifications [WWW]. Accessed on [22.09.2014]. Available at: http://www.huawei.com/ecommunity/bbs/10182143.html

[30] 3GPP. User Equipment (UE) Radio Access capabilities. 2011, TS 25.306 version 10.2.0 Release 10.

[31] Kathrein Ltd, 742210V01, 68° cross polarization multiband directional antenna.

[32] Ari Asp, Yaroslav Syorov, Mikko Keskikastari, Mikko Valkama and Jarno Niemelä. Impact of Modern Construction Materials on Radio Signal Propagation: Practical Measurements and Network Planning Aspects. Tampere University of Technology, Tampere.

[33] Ari Asp, Yaroslav Syorov, Mikko Valkama and Jarno Niemelä. Radio Signal Propagation and Attenuation Measurements for Modern Residential Buildings. The 4th IEEE International Workshop on Heterogeneous and Smart Cell Networks (HetSNets).

[34] Mobile Performance Gaming. Greatest Heroes Ltd. [WWW] Accessed on [18.10.2014]. Available at: http://www.greatestheroes.fi/about/

APPENDIX A

Appendix A presents the effects of user location on the RSRP signal levels at different corridors and rooms in each floor in terms of differences in the mean and median value of RSRP.

Table A.1. *Comparison table of RSRP values for different corridors.*

	CORRIDOR	POINT	RSRP gain [dB]		REMARKS
			MEAN	MEDIAN	
THIRD FLOOR	G corridor	Point 3	1.62	1.60	Moved over initial
			1.42	1.75	Moved over moving
			0.20	−0.15	Moving over initial
		Point 4	15.74	15.70	Middle over left
			7.45	7.40	Middle over right
			8.29	8.30	Right over left
	Corridor F	Point6	13.90	15.00	Middle over left
			14.53	15.20	Middle over right
			−0.63	−0.20	Right over left
	Corridor E	Point 8	4.43	4.40	Middle over left
			6.48	7.60	Middle over right
			−2.05	−3.00	Right over left
SECOND FLOOR	G corridor	Point 3	1.42	1.72	Moving over initial
			1.64	2.00	Moving over moved
			−0.22	−0.28	Moved over initial
		Point 4	−1.04	−1.80	Middle over left
			5.23	5.10	Middle over right
			−6.27	−6.90	Right over left
	Corridor F	Point6	5.04	5.30	Middle over left
			4.97	5.20	Middle over right
			0.07	0.10	Right over left
FOURTH FLOOR	G corridor	Point 4	8.20	9.20	Middle over left
			5.74	6.90	Middle over right
			2.46	2.30	Right over left
		Point 2	7.57	7.30	Middle over left
			2.98	3.00	Middle over right
			4.59	4.30	Right over left

Note: *Remarks such as "middle over left" means RSRP value at middle of the corridor is greater than the RSRP value at left side of the corridor.*

Table A.2. *Comparison table of RSRP values for different rooms.*

ROOM	RSRP gain [dB]		REMARKS
	MEAN	MEDIAN	
TG304	7.02	7.30	Door over corner
	7.91	8.20	Door over window
	0.89	0.90	Corner over window
TG206	1.19	1.10	Door over corner
	−0.29	−0.20	Door over window
	−1.48	−1.30	Corner over window
TG304	3.88	4.25	Door over corner
	7.49	4.50	Door over window
	3.61	0.25	Corner over window

APPENDIX B

Appendix B lists statistical values of the RSRP and SNR at all the measurement points.

I. TABLES FOR MEASUREMENTS IN THE CORRIDORS

THIRD FLOOR

Table B.1. *Calculated values of RSRP and SNR at point 3 of G corridor in third floor.*

	Value / Location	Min	Max	Mean	Median	s.d.	Max − Min
RSRP	**Initial location**	−83.70	−74.40	−79.05	−78.80	2.36	9.30
	Moving location	−84.50	−74.00	−78.85	−78.95	2.49	10.50
	Moved location	−81.10	−75.10	−77.43	−77.20	1.46	6.00
SNR	**Initial location**	21.90	29.40	27.03	28.00	2.07	7.50
	Moving location	19.40	29.40	26.05	27.30	3.15	10.00
	Moved location	26.30	29.50	28.12	28.10	0.73	3.20

Table B.2. *Calculated values of RSRP and SNR at point 4 of G corridor in third floor.*

	Value / Location	Min	Max	Mean	Median	s.d.	Max – Min
RSRP	**Left side**	−66.20	−61.70	−63.60	−63.50	0.98	4.50
	Right side	−58.00	−53.90	−55.31	−55.20	0.91	4.10
	Middle	−48.90	−47.20	−47.86	−47.80	0.39	1.70
SNR	**Left side**	17.60	29.60	25.26	28.50	4.77	12.00
	Right side	23.10	29.60	27.70	28.60	1.84	6.50
	Middle	27.40	29.70	28.85	28.90	0.52	2.30

Table B.3. *Calculated values of RSRP and SNR at point 6 of F corridor in third floor.*

	Value / Location	Min	Max	Mean	Median	s.d.	Max – Min
RSRP	**Left side**	−84.60	−75.00	−79.55	−79.40	2.27	9.60
	Right side	−86.80	−76.00	−80.18	−79.60	2.89	10.80
	Middle	−77.70	−63.20	−65.65	−64.40	3.44	14.50
SNR	**Left side**	9.10	28.70	22.04	24.80	6.58	19.60
	Right side	16.90	29.50	25.61	27.70	4.23	12.60
	Middle	27.60	29.70	28.89	29.10	0.57	2.10

Table B.4. *Calculated values of RSRP and SNR at point 8 of E corridor in third floor.*

	Value / Location	Min	Max	Mean	Median	s.d.	Max – Min
RSRP	**Left side**	−88.30	−75.90	−79.61	−79.00	2.94	12.40
	Right side	−88.10	−72.90	−81.66	−82.00	3.53	15.20
	Middle	−81.30	−72.20	−75.18	−74.60	2.30	9.10
SNR	**Left side**	15.00	23.10	19.50	19.70	2.03	8.10
	Right side	18.30	25.90	22.47	22.50	1.94	7.60
	Middle	20.10	27.40	23.89	24.20	2.16	7.30

Table B.5. *Calculated values of RSRP and SNR at point 2 of H corridor in third floor.*

	Value / Location	Min	Max	Mean	Median	s.d.	Max – Min
RSRP	**Left side**	−76.20	−71.50	−72.73	−72.40	1.02	4.70
	Right side	−78.90	−72.40	−74.98	−74.70	1.49	6.50
	Middle	−67.60	−37.50	−75.18	−61.40	8.07	30.1
SNR	**Left side**	24.00	29.00	27.24	27.20	1.32	5.00
	Right side	15.10	28.70	21.81	18.70	5.37	13.60
	Middle	12.60	29.20	23.74	22.30	4.77	16.60

SECOND FLOOR

Table B.6. *Calculated values of RSRP and SNR at point 3 of G corridor in second floor.*

	Value / Location	Min	Max	Mean	Median	s.d.	Max – Min
RSRP	**Initial location**	−108.80	−102.60	−105.62	−105.80	1.72	6.20
	Moving location	−106.80	−102.20	−104.20	−104.10	1.06	4.60
	Moved location	−112.00	−99.90	−105.84	−106.10	3.39	12.1
SNR	**Initial location**	7.10	15.20	11.18	11.20	2.05	8.10
	Moving location	4.10	15.20	9.49	9.00	3.12	11.10
	Moved location	8.70	14.90	12.88	13.10	1.28	6.20

Table B.7. *Calculated values of RSRP and SNR at point 4 of G corridor in second floor.*

	Value / Location	Min	Max	Mean	Median	s.d.	Max – Min
RSRP	**Left side**	−83.80	−75.20	−77.33	−76.50	2.22	8.60
	Right side	−88.80	−78.70	−83.60	−83.40	2.44	10.10
	Middle	−81.00	−76.10	−78.37	−78.30	0.92	4.90
SNR	**Left side**	23.80	29.30	28.16	28.80	1.45	5.50
	Right side	23.60	29.40	27.29	27.90	1.64	5.80
	Middle	12.50	29.10	23.57	28.50	6.05	16.60

Table B.8. *Calculated values of RSRP and SNR at point 6 of F corridor in second floor.*

	Value / Location	Min	Max	Mean	Median	s.d.	Max – Min
RSRP	**Left side**	−106.10	−101.00	−103.17	−103.20	1.05	5.10
	Right side	−106.70	−100.50	−103.10	−103.10	1.31	6.20
	Middle	−101.20	−96.00	−98.13	−97.90	1.10	5.20
SNR	**Left side**	15.00	19.60	17.91	18.30	1.14	4.60
	Right side	8.70	18.80	16.15	17.30	2.78	10.1
	Middle	18.80	25.40	22.97	23.60	1.91	6.6

FOURTH FLOOR

Table B.9. *Calculated values of RSRP and SNR at point 4 of G corridor in fourth floor.*

	Value / Location	Min	Max	Mean	Median	s.d.	Max – Min
RSRP	**Left side**	−89.60	−83.10	−86.39	−86.40	1.46	6.50
	Right side	−85.40	−81.50	−83.93	−84.10	0.85	3.90
	Middle	−85.30	−76.60	−78.19	−77.20	2.39	8.70
SNR	**Left side**	16.20	24.30	20.57	20.50	2.11	8.10
	Right side	24.50	27.90	26.13	26.20	0.89	3.40
	Middle	24.90	28.10	26.41	26.10	1.14	3.20

Table B.10. *Calculated values of RSRP and SNR at point 2 of H corridor in fourth floor.*

	Value / Location	Min	Max	Mean	Median	s.d.	Max − Min
RSRP	**Left side**	−108.40	−97.90	−101.33	−101.40	1.28	10.50
	Right side	−104.4	−90.10	−96.70	−97.10	1.39	14.30
	Middle	−98.50	−85.30	−93.66	−94.10	2.38	13.20
SNR	**Left side**	3.00	10.10	6.91	6.80	1.07	7.10
	Right side	5.60	14.90	10.17	10.40	1.27	9.30
	Middle	6.80	18.30	11.56	11.30	2.35	11.50

II. TABLES FOR MEASUREMENTS INSIDE ROOMS

Table B.11. *Calculated values of RSRP and SNR inside a room in third floor.*

	Value / Location	Min	Max	Mean	Median	s.d.	Max − Min
RSRP	**At corner**	−75.30	−69.70	−72.44	−72.40	1.34	5.60
	Near window	−75.00	−71.60	−73.33	−73.30	0.88	3.40
	Near door	−68.90	−63.70	−65.42	−65.10	1.13	5.20
SNR	**At corner**	26.40	29.80	28.91	29.00	0.61	3.40
	Near window	13.30	29.00	22.95	25.00	5.96	15.70
	Near door	27.30	29.70	28.66	28.70	0.57	2.40

TableB.12. *Calculated values of RSRP and SNR inside a room in second floor.*

	Value / Location	Min	Max	Mean	Median	s.d.	Max − Min
RSRP	**At corner**	−94.30	−87.90	−90.71	−90.60	1.53	6.40
	Near window	−91.70	−87.30	−89.23	−89.30	1.12	4.40
	Near door	−92.50	−86.80	−89.52	−89.50	1.21	5.70
SNR	**At corner**	23.10	27.20	25.53	25.60	0.98	4.10
	Near window	17.10	25.50	21.68	21.80	2.68	8.40
	Near door	17.30	26.70	21.68	21.40	3.08	9.40

Table B.13. *Calculated values of RSRP and SNR inside a room in fourth floor.*

	Value / Location	Min	Max	Mean	Median	s.d.	Max − Min
RSRP	**At corner**	−89.20	−85.00	−87.78	−87.95	0.97	4.20
	Near window	−115.30	−86.70	−91.39	−88.20	8.74	28.6
	Near door	−86.90	−82.20	−83.90	−83.70	0.89	4.7
SNR	**At corner**	21.70	26.50	24.38	24.70	1.29	4.80
	Near window	3.20	25.80	16.79	15.20	6.55	22.60
	Near door	22.60	27.90	25.86	26.30	1.46	5.30

APPENDIX C

Appendix C presents the maximum difference between the weakest and strongest values of the received signal strength levels. These differences are denoted by blue color and red color for RSRP and SNR, respectively.

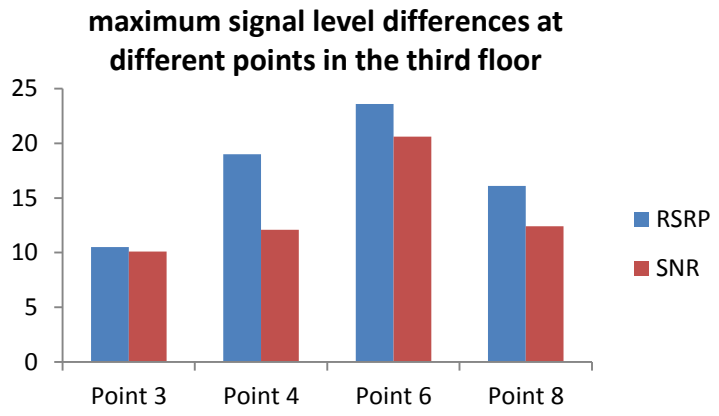

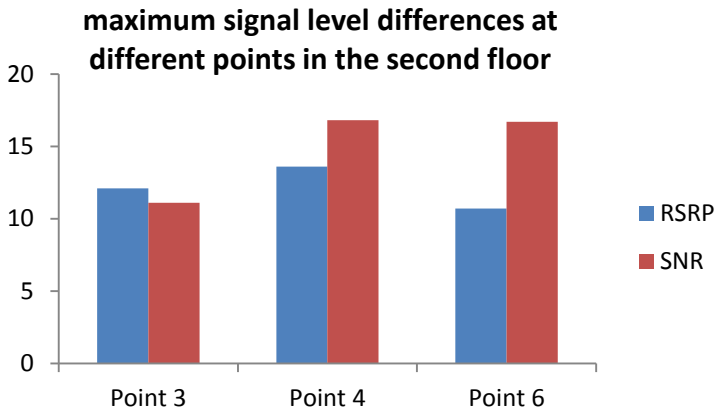

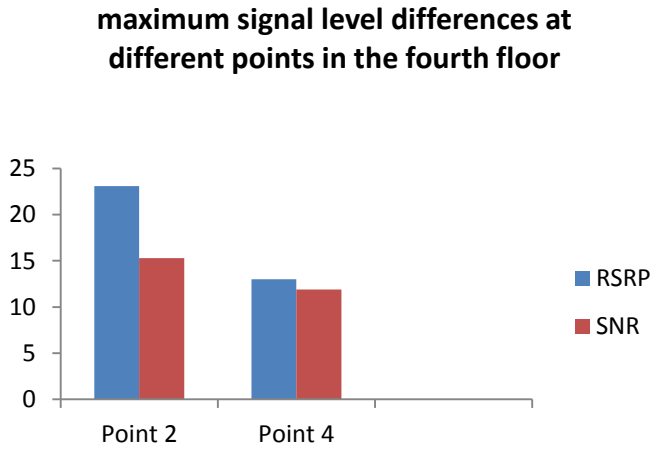

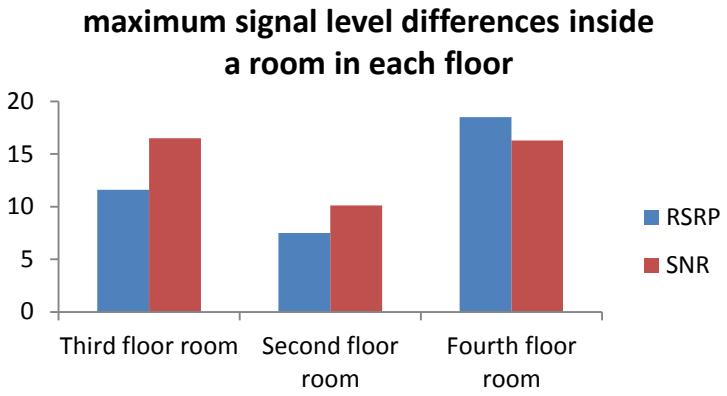
maximum signal level differences inside a room in each floor
20
15
10
5
0
Third floor room
Second floor room
Fourth floor room
RSRP
SNR